Firearm Injuries and Illicit Drug Markets:
An Econometric Analysis of Costs, Violence, and Spatial Dependence

Ronald Dickerson

A dissertation
submitted in partial fulfillment of the
requirements for the degree of

Doctor of Philosophy

University of Washington
2026

Reading Committee:

Anirban Basu, Chair

Ali Rowhani-Rahbar

Jing Li

Program Authorized to Offer Degree:

Pharmacy

University of Washington

Abstract

Firearm Injuries and Illicit Drug Markets:
An Econometric Analysis of Costs, Violence, and Spatial Dependence

Ronald Dickerson

Chair of the Supervisory Committee:
Anirban Basu
Pharmacy

Firearm violence imposes a large and deeply unequal burden on the United States, yet the evidence base for policy remains fragmented. Two gaps are especially consequential. First, medical costs of firearm injury are typically reported at national or state levels that obscure the local variation relevant for trauma-system planning and geographic payment policy. Second, the upstream market conditions associated with lethal firearm violence remain incompletely understood. This dissertation addresses both gaps by combining insurance claims, public health surveillance, and economic data with spatial and causal inference methods to improve how firearm-related harm is measured and interpreted for policy.

The first aim estimates a population-calibrated, county-level surface of mean 30-day treatment cost per treated firearm injury patient in the United States from 2016 through 2024. Using longitudinal claims from the Komodo Healthcare Map (N = 10,343 treated patients), the analysis constructs survival-adjusted episode costs, corrects for uneven claims coverage using inverse-probability weighting benchmarked to the American Community Survey, and recovers stable small-area estimates through Bayesian spatiotemporal smoothing. The case-weighted national mean predicted 30-day treatment cost was $67,275 per treated patient, and the case-weighted median was $66,985. Across counties, treatment costs were regionally organized rather than randomly distributed: raw county costs were highly dispersed, annual P90/P10 ratios ranged from 2.3 to 3.4 before smoothing, and costs were strongly spatially clustered (Moran's I, 0.583), remaining correlated across an estimated 222 km. In a sequential decomposition, adjustment for local Medicare reimbursement geography was associated with the largest single-step reduction in geographic inequality, with the mean annual county P90/P10 ratio declining from 1.86 to 1.69. Additional adjustment for payer mix and insurance-market structure reduced the ratio to 1.59, and further adjustment for demographic composition, injury burden,

deprivation, local violence burden, health care capacity, and regional utilization norms reduced the ratio to 1.51 in the fully adjusted model. These findings suggest that payment geography and local financing conditions are important, but incomplete, sources of geographic variation in paid firearm injury treatment costs. The remaining variation should not be interpreted as county-level inefficiency; it may reflect unmeasured injury severity, frailty, payer contracts, referral patterns, coding intensity, or regional delivery-system organization.

The second aim examined whether exogenous changes in illicit drug prices affected firearm homicide rates in six high-exposure US cities — Dallas, Houston, Los Angeles, Phoenix, San Antonio, and San Diego — observed annually from 2016 through 2023 (N = 48 city-years). Sparse Drug Enforcement Administration transaction data were converted into complete city-year price signals through a drug-specific spatiotemporal recovery model with explicit instrument separation, then aggregated into integrated, opioid, and stimulant drug-price indices. Panel instrumental-variables models used log seizures as the excluded instrument. First-stage statistics were strong across specifications (F = 28 to 520), and placebo and falsification tests detected no evidence that instrumented drug-price variation was associated with enforcement intensity, pre-existing homicide trends, or broad non-drug-market shocks. Instrumented drug prices were negatively associated with firearm homicide across all three indices, with point estimates ranging from −0.68 to −2.85 on the log firearm homicide rate. The stimulant price specification produced the clearest evidence of a negative association, while integrated and opioid price estimates were negative but less precise. Spatial robustness checks produced broadly similar point estimates but wider uncertainty for the integrated and opioid specifications. These results do not support the hypothesis that higher illicit drug prices increased firearm homicide in this high-exposure US city sample, although the design cannot identify the specific mechanism linking price changes to violence.

Together, these aims provide a new empirical foundation for local trauma-system planning and geographic payment calibration, advance spatial and causal methods for recovering interpretable structure from sparse and nonrepresentative data, and connect the downstream medical costs of firearm injury to the broader economic environments in which firearm violence occurs. The dissertation treats firearm harm simultaneously as a health care system burden — organized regionally and shaped by payment geography and delivery-system capacity — and as a geographically structured consequence of upstream economic and institutional environments.

Acknowledgments

I am deeply grateful to my chair, Anirban Basu, for his mentorship, intellectual rigor, and steady encouragement throughout my doctoral training. His guidance pushed me to think more clearly, write more carefully, and approach research with greater discipline and ambition.

I am sincerely grateful to Jing Li for her thoughtful feedback, methodological insight, and generosity with her time. Her close reading of my work and consistent emphasis on clarity and precision substantially strengthened this dissertation. I am also very thankful to Ali Rowhani-Rahbar for his guidance, subject-matter expertise, and support in shaping this work at the intersection of injury research, policy, and population health.

I am grateful to the faculty, staff, and students of the Comparative Health Outcomes, Policy, and Economics (CHOICE) Institute and the University of Washington School of Pharmacy for providing an exceptional intellectual home. I especially appreciate the support of colleagues, mentors, and collaborators who offered feedback, conversation, and encouragement throughout this process.

This dissertation benefited from access to multiple data resources. I am grateful for the use of the Komodo Healthcare Map, the American Community Survey, County Health Rankings, the Dartmouth Atlas of Health Care, and Centers for Medicare & Medicaid Services geographic payment files. I also acknowledge the Drug Enforcement Administration Freedom of Information and Privacy Act Unit for processing my request and releasing the STRIDE spreadsheet that supported the dissertation’s second aim.

Finally, I thank my family, friends, and loved ones for their patience, encouragement, and belief in me throughout graduate school. Their support sustained me through the most difficult and uncertain parts of this journey. This dissertation reflects not only my own effort, but also the generosity and faith of the people who stood behind me.

Table of Contents

List of Figures

List of Tables

Chapter 1

General Introduction

Firearm-Related Harm as a Spatially Organized Health-Economic Problem

Background and Significance

In 2023, 17,927 people in the United States died from firearm homicide. Many more survived firearm assaults and entered the health care system. Estimated nonfatal emergency department visits for firearm assaults increased from 50,482 in 2016 to 120,550 in 2023 — a 139% increase, or roughly 10,000 additional visits per year.[1] Fatal and nonfatal firearm injuries together impose an estimated $500 billion in annual societal costs, including direct medical spending for injuries that reach emergency or inpatient care.[2,3] These numbers identify firearm violence simultaneously as a mortality problem, a health care financing problem, and a local service-delivery problem.

Two basic features of that burden remain insufficiently characterized for policy. First, medical costs are still reported mainly at national or state scales. Aggregate estimates describe total burden but cannot identify counties where expected treatment costs are unusually high, cannot separate variation driven by reimbursement geography from variation driven by clinical need or care capacity, and cannot support the local trauma-system and payment decisions that depend on small-area patterns.[4-7] A national mean cannot tell a trauma-system planner whether their county's cost burden is elevated, whether nearby counties face similar pressures, or whether observed differences reflect efficient care, unusual injury severity, local price levels, early mortality, or sparse data.

The financing implications compound this problem. The U.S. Government Accountability Office estimated that initial hospital costs for firearm injuries exceeded $1 billion annually in 2016 and 2017, excluding physician fees that could add roughly another 20 percent. Medicaid and other public coverage accounted for more than 60 percent of those costs, with Medicaid alone accounting for approximately half.[8] These figures cover initial hospitalization rather than the 30-day episode costs estimated in this dissertation, but they underscore why local variation in treatment costs matters for public payers, trauma systems, safety-net hospitals, and uncompensated-care financing.

Second, the upstream economic environments that shape lethal firearm violence remain causally unsettled. Illicit drug markets are one plausible contributor, especially in the synthetic-opioid era. The U.S. drug market has shifted from prescription opioid exposure toward illicit fentanyl, counterfeit pills, and multi-product trafficking networks. In this dissertation, drug prices serve as a market-level signal of local supply scarcity: when supply tightens relative to demand, prices rise. I recover this signal from DEA transaction data and use seizure-based supply shocks to isolate price variation plausibly driven by changes in supply rather than by local violence or enforcement responses. Higher drug prices could increase firearm violence by intensifying competition over territory and supply, or reduce it by contracting market activity and cutting the number of contested transactions.[9-14] Theory does not determine the sign; it must be estimated.

This dissertation addresses both gaps by combining insurance claims, public health surveillance, and economic data with spatial and causal inference methods designed to recover interpretable structure from imperfect data. Aim 1 produces a county-level surface of mean 30-day treatment costs per treated firearm-injury patient. Aim 2 estimates whether exogenous changes in illicit drug prices affect firearm homicide in six high-exposure U.S. cities during the 2016–2023 fentanyl restructuring era. Together, the aims treat firearm-related harm as a spatially organized health-economic problem: one that begins in social and market environments, produces injury and death, and then enters regional health care systems through trauma care, payment, and post-injury treatment.

Conceptual Framework

The dissertation is organized around a downstream–upstream framework. Aim 1 studies one downstream consequence of firearm injury: the paid medical costs generated after a patient survives to receive emergency or inpatient care. Aim 2 studies one upstream economic environment that may shape whether firearm violence occurs: local illicit drug prices. The aims are conceptually paired but not causally linked. They share three structural features that motivate joint treatment.

First, both aims confront sparse and nonrepresentative data. Aim 1 uses claims with detailed cost information but uneven payer and geographic coverage; Aim 2 uses DEA transaction records with informative price signals but observations in only a minority of city-year-drug cells. Both therefore require model-based recovery of local quantities that cannot be reliably estimated from direct observation alone.

Second, both aims treat geography as substantive rather than as a nuisance. Treatment costs cluster regionally because trauma systems, referral networks, payer geography, and health care capacity are spatially organized. Firearm homicide may cluster regionally because drug markets, trafficking corridors, and enforcement environments cross city boundaries. Spatial dependence is part of the phenomenon being studied in both aims, not a modeling artifact to be absorbed and set aside.

Third, both aims accommodate directional ambiguity in their estimands. In Aim 1, lower observed costs can indicate efficient treatment, less severe injury, early mortality, or limited access; higher costs can reflect more intensive care, greater survival, higher local prices, or more severe case mix. In Aim 2, higher drug prices could either intensify violence through territorial conflict or reduce it through market contraction. The dissertation treats both directions as empirical questions and reports findings without assuming which direction is normatively desirable.

Specific Aims

Aim 1. Estimate county-level 30-day firearm-injury treatment costs and characterize geographic structure

Using longitudinal insurance claims from the Komodo Healthcare Map (N = 10,343 treated patients, 2016–2024), the analysis constructs survival-adjusted episode costs using a Kaplan–Meier sample average estimator, corrects for uneven claims coverage using inverse-probability weighting benchmarked to the American Community Survey, and recovers stable small-area estimates through Bayesian spatiotemporal smoothing using the Stochastic Partial Differential Equation approach to Integrated Nested Laplace Approximation.[15-17] Aim 1 addresses four research questions: (1) How are county-level firearm-injury treatment costs distributed across the United States? (2) How much of the observed geographic inequality is associated with local Medicare reimbursement geography, demographic composition, injury burden, health-care capacity, and utilization norms, and at what stage of a sequential decomposition does each block enter? (3) What is the estimated regional scale of cost clustering? (4) After full adjustment, do counties with higher local homicide burdens have distinguishable residual treatment-cost patterns?

The primary estimand is the county-specific mean 30-day treatment cost per treated firearm-injury patient, conditional on surviving to receive emergency or inpatient care and on having sufficient claims observability for episode construction. It is not an estimate of total societal burden or the cost of all firearm injuries.

Aim 2. Estimate the effect of drug prices on firearm homicide in high-exposure U.S. cities

The second aim examines six high-exposure U.S. cities — Dallas, Houston, Los Angeles, Phoenix, San Antonio, and San Diego — observed annually from 2016 through 2023. The analysis constructs city-year drug price indices from sparse DEA STRIDE transaction data using a drug-specific spatiotemporal recovery step that explicitly separates price recovery from the seizure-based instruments used for identification. Panel instrumental-variables models then estimate the effect of recovered drug prices on the log firearm homicide rate, using log drug seizures as the excluded instrument. Tiered spatial robustness checks compare panel two-stage least squares estimates against INLA models with temporal random effects and against INLA models with a continuous-space Matérn spatial field. Placebo and falsification tests assess the seizure instrument against enforcement-intensity outcomes, lagged firearm homicide, and a non-drug-market falsification outcome.

The analysis does not assume a directional effect. Four working hypotheses organize the design: (1) seizure-based supply shocks predict the recovered city-year drug price indices in high-exposure cities; (2) instrumented drug prices affect firearm homicide, with the sign left open because market-conflict and market-contraction mechanisms point in opposite directions; (3) firearm homicide exhibits residual spatial dependence after conditioning on city and year fixed effects; and (4) incorporating spatial structure improves model fit and reduces residual spatial autocorrelation. The primary estimand is the local average treatment effect of a one-standard-deviation increase in the instrumented integrated drug-price index on the log firearm homicide rate, for complier cities in the high-exposure sample.

Innovation

The dissertation makes three principal contributions.

First, it produces a county-level treatment-cost surface for firearm injury with explicit uncertainty quantification. Prior cost studies have established that firearm injuries are expensive but have not delivered local estimates usable for trauma planning, payment evaluation, or surveillance. The integrated workflow — combining population calibration, censoring adjustment, geographic harmonization, and Bayesian spatiotemporal smoothing — addresses several common limitations of claims-based small-area estimation in a single analysis.

Second, it applies a causal-inference framework suited to the synthetic-opioid era to the drug price–firearm homicide relationship. Stage 0 instrument separation prevents the excluded instrument from being mechanically embedded in the constructed exposure. The agnostic hypothesis framing accommodates a genuinely ambiguous theoretical prediction, and the tiered spatial robustness approach quantifies the impact of residual spatial dependence on inference.

Third, the dissertation treats spatial dependence as substantive empirical evidence across both aims. In Aim 1, treatment costs cluster at a regional scale of approximately 222 km. In Aim 2, residual spatial dependence in firearm homicide is present and structured. In both cases, the relevant signal exceeds neighborhood scales — suggesting that firearm-related harm operates at regional rather than purely local levels, and that administrative boundaries are often the wrong unit for inference about trauma planning or violence prevention.

Significance

For health economics and outcomes research, the dissertation demonstrates how Bayesian spatiotemporal methods can recover interpretable local quantities from sparse, nonrepresentative data — a problem endemic to firearm research, where high-acuity events are concentrated and surveillance systems are uneven.

For firearm-injury policy, Aim 1 provides a local empirical baseline that trauma systems and payers can use to identify counties where expected treatment costs are atypically high, where uncertainty is large, and where additional data linkage could improve regional planning. Aim 2 speaks directly to whether supply-side enforcement in the synthetic-opioid era produces collateral firearm-violence harms or benefits — a question that remains open in current drug-policy debates.[13]

For spatial methods in public health, the dissertation shows that residual spatial dependence is a feature of both firearm-injury treatment costs and firearm homicide rates, that it operates at regional rather than neighborhood scales in both phenomena, and that ignoring it can mischaracterize geographic inequality and the precision of estimated effects.

Dissertation Structure

Chapter 2 presents Aim 1, including data construction, inverse-probability weighting, Kaplan–Meier sample-average adjustment, sequential covariate decomposition, Bayesian spatiotemporal smoothing, and sensitivity analyses. Chapter 3 presents Aim 2, including Stage 0 price recovery, instrumental-variables analysis, placebo and falsification tests, and tiered spatial robustness checks. Chapter 4 synthesizes the findings from both aims, describes their joint implications for health economics, public policy, and spatial methods, identifies cross-cutting limitations, and outlines directions for future research.

References

1. Centers for Disease Control and Prevention. WISQARS Fatal Injury Data. Accessed 2024.
2. Peterson C, Luo F, Florence C. State-level economic costs of fatal injuries — United States, 2019. *MMWR Morb Mortal Wkly Rep*. 2021;70:1660–1663.
3. Miller GF, Barnett SBL, Florence CS, McDavid Harrison K, Dahlberg LL, Mercy JA. Costs of fatal and nonfatal firearm injuries in the U.S., 2019 and 2020. *Am J Prev Med*. 2024;66(2):195–204.
4. Ranney ML, Herges C, Metcalfe L, et al. Increases in actual health care costs and claims after firearm injury. *Ann Intern Med*. 2020;173(12):949–955.
5. Spitzer SA, Staudenmayer KL, Tennakoon L, Spain DA, Weiser TG. Costs and financial burden of initial hospitalizations for firearm injuries, 2006–2014. *Am J Public Health*. 2017;107(5):770–774.
6. Cook A, Osler T, Hosmer D, et al. Gunshot wounds resulting in hospitalization in the United States: 2004–2013. *Injury*. 2017;48(3):621–627.
7. Royan R, Lundberg A, Shan Y, Thomas AC, Stey AM. Health care costs of firearm injury hospital visits in the US. *JAMA Health Forum*. 2025;6(9):e253299.
8. US Government Accountability Office. Firearm Injuries: Health Care Service Needs and Costs. GAO-21-515. Washington, DC: US Government Accountability Office; 2021.
9. Goldstein PJ. The drugs/violence nexus: a tripartite conceptual framework. *J Drug Issues*. 1985;15(4):493–506.
10. Martínez R, Rosenfeld R, Mares D. Social disorganization, drug market activity, and neighborhood violent crime. *Urban Aff Rev*. 2008;43(6):846–874.
11. Castillo JC, Mejía D, Restrepo P. Scarcity without Leviathan: the violent effects of cocaine supply shortages in the Mexican drug war. SSRN Working Paper; 2018. DOI: 10.2139/ssrn.2409268.
12. DeSimone J. The effect of cocaine prices on crime. *Econ Inq*. 2001;39(4):627–643.
13. Friedman J, Ciccarone D. The public health risks of counterfeit pills. *Lancet Public Health*. 2025;10(1):e58–e62.
14. Caulkins JP. How should drug policy respond to surging supplies of dangerous drugs? Brookings Institution; December 2024.
15. Basu A, Manning WG. Estimating lifetime or episode-of-illness costs under censoring. *Health Econ*. 2010;19(9):1010–1028.
16. Lindgren F, Rue H, Lindström J. An explicit link between Gaussian fields and Gaussian Markov random fields: the SPDE approach. *J R Stat Soc B*. 2011;73(4):423–498.
17. Lindgren F, Rue H. Bayesian spatial modelling with R-INLA. *J Stat Softw*. 2015;63(19):1–25.

Chapter 2

County-Level 30-Day Firearm Injury Treatment Costs in the United States:

Implications for Trauma-System Planning and Payment Geography

Ronald Dickerson, MA, MPH, Jing Li, PhD, Ali Rowhani-Rahbar, MD, PhD, Anirban Basu, PhD

Key Points

Question How are county-level mean 30-day treatment costs per treated firearm injury patient distributed across US counties, and how much of the observed geographic inequality is associated with local Medicare reimbursement geography and measured demographic, contextual, and health care system factors?

Findings In this retrospective cohort study of 10,343 treated firearm injury patients from 2016 through 2024, the case-weighted national mean predicted 30-day treatment cost was $67,275 per treated patient. County-level costs were strongly spatially clustered (Moran's I, 0.583) and remained correlated over an estimated 222 km. Adjustment for local Medicare reimbursement geography produced the largest single-step reduction in geographic inequality, with the mean annual county-level P90/P10 ratio declining from 1.86 to 1.69; further adjustment for payer mix, insurance-market structure, demographic composition, injury burden, deprivation, local violence burden, health care capacity, and utilization norms reduced the ratio to 1.51.

Meaning Local Medicare payment geography and payer-market structure were associated with meaningful but incomplete reductions in regional variation in predicted county-level costs. After full adjustment, counties near the top of the cost distribution still had predicted costs approximately 51% higher than counties near the bottom. The remaining variation may reflect regional delivery-system organization, unmeasured injury severity and case mix, or both. The resulting county-level cost surface may inform regional trauma-system planning, evaluation of geographic payment adjustment, and surveillance of local firearm-injury treatment costs and data gaps.

Abstract

Importance. Firearm injuries impose substantial medical and societal costs in the United States, yet existing cost estimates are reported almost exclusively as national or state-level totals. Those summaries obscure how treatment costs are distributed across local areas and limit their usefulness for trauma-system planning, geographic payment policy, and surveillance.

Objective. To estimate county-level mean 30-day treatment cost per treated firearm injury patient across the United States and assess how much geographic inequality is associated with local Medicare reimbursement geography and measured payer-market, demographic, contextual, and health care system factors.

Design. Retrospective cohort study.

Setting. Longitudinal insurance claims from the Komodo Healthcare Map, January 1, 2016, through December 31, 2024.

Participants. Patients with treated firearm injuries who survived to receive emergency department or inpatient care and met enrollment criteria for 30-day episode construction.

Exposure. County of residence and county-level local Medicare reimbursement geography, payer mix and insurance-market structure, demographic composition, injury burden, deprivation, local violence burden, health care capacity, and utilization characteristics.

Main Outcomes and Measures. Mean 30-day treatment cost per treated firearm injury patient, in 2024 US dollars. Claims were calibrated to local population benchmarks using inverse-probability weighting, adjusted for administrative censoring, smoothed using a Bayesian spatiotemporal model, and allocated from 3-digit ZIP code areas to counties using population-weighted fractional crosswalk methods. Geographic inequality was summarized using the P90/P10 ratio of predicted county costs across 7 sequential models.

Results. Among 10,343 patients with treated firearm injuries, raw county-level treatment costs were highly dispersed and spatially clustered (Moran’s I, 0.583; $P < .001$), with annual P90/P10 ratios ranging from 2.3 to 3.4 before smoothing. The case-weighted national mean predicted

30-day treatment cost was $67,275 per treated patient; the case-weighted median was $66,985 (interquartile range, $64,340–$70,525). The estimated spatial correlation range was 222 km (95% credible interval, 197–250 km). In the as-observed prediction surfaces, the mean annual county P90/P10 ratio declined from 1.86 at baseline to 1.69 after adjustment for local Medicare reimbursement geography, 1.59 after additional adjustment for payer mix and insurance-market structure, and 1.51 in the fully adjusted model. In standardized surfaces, the corresponding ratio declined from 1.85 to 1.68, 1.57, and 1.50. Holdout validation showed strong agreement between predicted and observed costs (Pearson $\rho = 0.90$; root mean squared error, $1,050). Thirty-day mortality was 1.1% and geographically sparse.

Conclusions and Relevance. Local Medicare payment geography and payer-market structure were associated with meaningful but incomplete reductions in geographic inequality in 30-day firearm injury treatment costs. Substantial regional variation remained after adjustment for measured demographic, contextual, and health care system factors, with counties near the top of the cost distribution having predicted costs approximately 51% higher than counties near the bottom. Residual variation may reflect regional delivery-system organization, unmeasured injury severity and frailty, payer contracts, or other unmeasured case-mix and system factors. These findings provide a county-level baseline that may inform trauma-system planning, geographic payment calibration, and firearm-injury surveillance.

Introduction

Firearm injuries impose substantial and growing costs on the US health care system. The annual societal cost of firearm violence exceeds $500 billion, including direct medical spending, lost productivity, and quality-of-life losses. Within the health care sector, direct medical expenditures among individuals who receive emergency or inpatient care are estimated at approximately $11 billion annually, while hospital-based costs alone were estimated at $7.7 billion nationally from 2016 through 2021.[1-3] Inpatient care accounts for more than 90% of initial hospital expenditures, and nonfatal injuries disproportionately affect young men, racial and ethnic minorities, and residents of the South.[2-4] Despite this scale, available cost estimates are almost entirely national or state-level totals — a level of aggregation at which variation across local areas is largely invisible.

That limitation matters because decisions about trauma care are made locally and regionally. Trauma-system planning, regional capacity investment, and geographic payment policy all depend on where care is delivered and how its costs vary across places. No population-calibrated, county-level map of mean 30-day firearm injury treatment costs currently exists for the United States. Without local evidence, geographic differences in spending are difficult to interpret: lower costs in a county may reflect lower treatment intensity, but they may also reflect lower survival to care, limited local capacity, a less severe case mix, or differences in local payment geography. Treating any one of these explanations as sufficient without evidence can lead to planning and payment errors that affect access and capacity in communities most affected by firearm violence.[5-7]

This question fits within a longer-standing literature on geographic variation in US health care spending. Wennberg and Fisher and colleagues documented that regional differences in Medicare spending persist after adjusting for prices and illness burden, with much of the residual variation reflecting differences in utilization, supply-sensitive care, and local practice style rather than population health needs.[8,9] Subsequent work has shown that geographic price adjustment narrows but does not eliminate these differences, and that a substantial share of the remaining variation traces to place-specific delivery-system factors rather than to the characteristics of the patients themselves.[10,11] We extend this framework to high-acuity firearm-injury episodes by estimating a county-level treatment-cost surface and decomposing geographic inequality across payment, payer-mix, population, injury-burden, capacity, and utilization domains.

We estimated a national county-level surface of mean 30-day treatment cost per treated firearm injury patient and examined how much of the observed geographic inequality was associated with local Medicare reimbursement geography, payer mix and insurance-market structure, demographic composition, injury burden, deprivation, local violence burden, health care capacity, and utilization norms. The analysis was descriptive. Residual geographic variation after adjustment may be consistent with regional delivery-system organization, but it may also reflect unmeasured differences in injury severity and case mix that the available data cannot distinguish.

Methods

Study Design and Data Sources

This study followed the Strengthening the Reporting of Observational Studies in Epidemiology (STROBE) reporting guideline. We conducted a retrospective cohort study of firearm injury treatment costs using longitudinal medical and pharmacy claims from the Komodo Healthcare Map (2016–2024). Komodo provides claims for approximately 330 million individuals across public and private payers; costs represent insurer-paid amounts across emergency, inpatient, outpatient, and pharmacy settings. We linked these claims to population benchmarks from the American Community Survey (ACS); county health and social measures from County Health Rankings (CHR; Robert Wood Johnson Foundation and University of Wisconsin Population Health Institute); regional health care system measures from the Dartmouth Atlas of Health Care; annual CMS Hospital Wage Index and Physician Geographic Practice Cost Index (GPCI) files to capture local Medicare reimbursement geography; and geographic crosswalk files to align data across reporting units. The full covariate inventory is provided in eTable 1 in the Supplement. Geographic harmonization methods are described in eMethods 1 in the Supplement. This study used deidentified insurance claims and was determined to be exempt from institutional review board oversight.

Cohort Definition

We identified patients with a treated firearm injury in emergency department or inpatient settings. Firearm injuries were defined using a validated set of ICD-10-CM external cause codes covering unintentional, assault-related, and undetermined-intent injuries.[16-20] We required a 180-day lookback period without a prior firearm injury diagnosis, active insurance coverage on the index date, and 30 days of observable claims follow-up. The final cohort comprised patients who survived to receive emergency or inpatient care and had insurance enrollment sufficient for 30-day episode observation. Patients without continuous preindex enrollment, those who died before reaching a facility, and those with insufficient follow-up were excluded. Cohort construction steps are shown in eTable 2 in the Appendix.

Outcome

The primary outcome was the mean 30-day treatment cost per treated firearm injury patient, in 2024 US dollars. Episode costs included all insurer-paid spending across inpatient, outpatient, emergency, and pharmacy settings in the 30 days after the index encounter. All payments were converted to 2024 dollars using the medical care component of the Consumer Price Index.[21]

Population Calibration and Censoring Adjustment

Claims coverage in Komodo varies by geography and payer, tending to overrepresent patients with stable commercial insurance and underrepresent Medicaid enrollees and those with intermittent coverage. We used inverse-probability weighting to align the claims cohort with local ACS population benchmarks on age, sex, insurance type, and ZIP3.[12,13-15] Some patients' insurance coverage ended before their 30-day window closed; we applied the Kaplan-Meier sample average estimator to estimate expected 30-day costs without understating spending among patients with early disenrollment.[22]

Spatial Modeling and County Allocation

Many ZIP3 areas had too few observed firearm injury cases for reliable direct cost estimates. We used a Bayesian spatiotemporal model to estimate a stable cost surface across all ZIP3 areas — stabilizing estimates in data-sparse areas by borrowing information from nearby areas and adjacent years and producing explicit uncertainty estimates at every location.[23-25] ZIP3-level predictions were then allocated to counties using population-weighted fractional crosswalk files that assign each ZIP3's predicted cost to overlapping counties in proportion to resident population share, preserving geographic continuity rather than imposing hard administrative borders.[13-15] Full technical details of the mesh construction, prior specifications, and temporal model structure are provided in eMethods 2 in the Appendix.

Sequential Decomposition of Geographic Cost Variation

The sequential models were designed as a descriptive decomposition of geographic cost variation, not as a causal mediation analysis. Covariate blocks were selected to represent contextual domains that prior health care spending-variation literature and trauma-system theory suggest may shape paid 30-day treatment costs: local reimbursement geography, payer mix and insurance-market structure, demographic composition, injury burden, deprivation and local violence burden, health care capacity, and regional utilization norms. Each block was interpreted as a contextual proxy for a hypothesized source of geographic variation in paid treatment costs, rather than as a confounder or mediator in a single causal pathway.

Model 1 included only the spatiotemporal structure, establishing the baseline geographic dispersion against which subsequent adjustments were evaluated. Model 2 added local Medicare reimbursement geography, measured using the CMS hospital wage index and physician practice expense GPCI, under the hypothesis that paid hospital and professional amounts partly reflect local input prices and administered payment rates in addition to treatment intensity. Model 3 added payer mix and insurance-market structure, including ACS-derived Medicaid, commercial insurance, and uninsured shares, as well as Medicare Advantage market concentration, to capture local financing conditions that may shape negotiated rates, public-payer payment levels, cross-subsidization, and uncompensated-care burdens. Model 4 added demographic composition, including sex and age structure, because these characteristics may correlate with firearm-injury patterns, survival to treatment, comorbidity, and treatment pathways. Model 5 added injury burden, deprivation, and local violence burden, including injury death rate, drug overdose mortality, county homicide rate, poverty, unemployment, and severe housing problems. These measures were included as proxies for broader clinical need, violent-injury exposure, social risk, and access barriers that may affect injury severity, survival to treatment, discharge planning, and follow-up care. Model 6 added health care capacity, including hospital beds, registered nurses, surgeons, emergency physicians, and critical care physicians per population, under the hypothesis that local trauma-capable infrastructure shapes the availability and intensity of acute care. Model 7 added utilization norms, including ambulatory care–sensitive, medical, and surgical discharges per population, reflecting the geographic-variation literature's finding that regional practice style and care intensity may shape spending beyond measured need, capacity, and prices.[8-11]

Geographic inequality was summarized using the P90/P10 ratio of predicted county costs—the ratio of the 90th to the 10th percentile—where a value of 2.0 indicates that counties near the top of the distribution have predicted costs twice as high as counties near the bottom. Changes in the county-level P90/P10 ratio across models were interpreted as the extent to which each contextual domain was descriptively associated with geographic inequality in predicted costs. Because the blocks are not orthogonal and the ordering reflects a prespecified sequence from payment geography and financing conditions to population context, local burden, system capacity, and practice-style measures, attenuation at any step should not be interpreted as the causal contribution of that block alone. Residual variation was not interpreted as inefficiency; it may reflect unmeasured injury severity, frailty, coding intensity, referral patterns, payer contracts, or regional delivery-system organization.[8-11]

Model Validation

We assessed interpolation performance in ZIP3 areas not used for model fitting, restricting the holdout sample to areas with at least 30 observed patients (80/20 training-to-holdout split). Agreement was measured using the Pearson correlation and root mean squared error between predicted and observed ZIP3 mean costs.

Results

Cohort and Geographic Coverage

The analytic cohort included 10,343 treated firearm injury patients from 2016 through 2024. Firearm injury encounters were identified in 85% of US ZIP3 areas, representing approximately 98% of the US population. Only 30% of ZIP3 areas had at least 10 observed encounters over the study period, supporting the use of spatial smoothing to generate stable small-area estimates. County-level encounter rates and the ZIP3 case-volume distribution are shown in eFigures 2.1 and 2.2 in the Appendix.

Spending Composition

Table 2.1 presents 30-day episode spending decomposed by care setting for the 2024 treated cohort. Inpatient care accounted for 58% of total spending and was concentrated among the 7.1% of patients who required hospitalization. Outpatient care and pharmacy spending were smaller in aggregate but were incurred by nearly all patients. These patterns indicate that the 30-day episode measure captured spending across the broader postinjury treatment course rather than hospitalization alone.

Table 2.1. Decomposition of 30-Day Episode Spending by Care Setting, 2024 Treated Cohort.

Care Setting	Total 30-Day Spending	Share of Total	Patients With Any Use	Share of Patients
Inpatient	$210,383,662	58%	109	7.1%
Outpatient	$100,654,270	28%	1,356	88.7%
Pharmacy	$52,682,205	14%	1,489	97.5%
Total	**$363,720,137**	**100%**	**1,528**	**100%**

Notes. Spending decomposed using within-patient care-setting shares from line-level claims. Results reflect the 2024 treated cohort and should not be interpreted as national annual burden estimates.

Population Calibration and Validation

Inverse-probability weighting substantially reduced demographic imbalance, with the maximum standardized difference declining from 0.20 before weighting to 0.08 after weighting and minimal loss of effective sample size (ratio, 0.99). In holdout validation, predicted and observed ZIP3 mean costs showed strong agreement (Pearson $\rho = 0.90$; 95% CI, 0.87–0.93; RMSE, \$1,050; 95% CI, \$899–\$2,650) (**Figure 2.1**).

Figure 2.1. ZIP3 holdout validation of the spatiotemporal smoothing model, United States, 2016–2024.

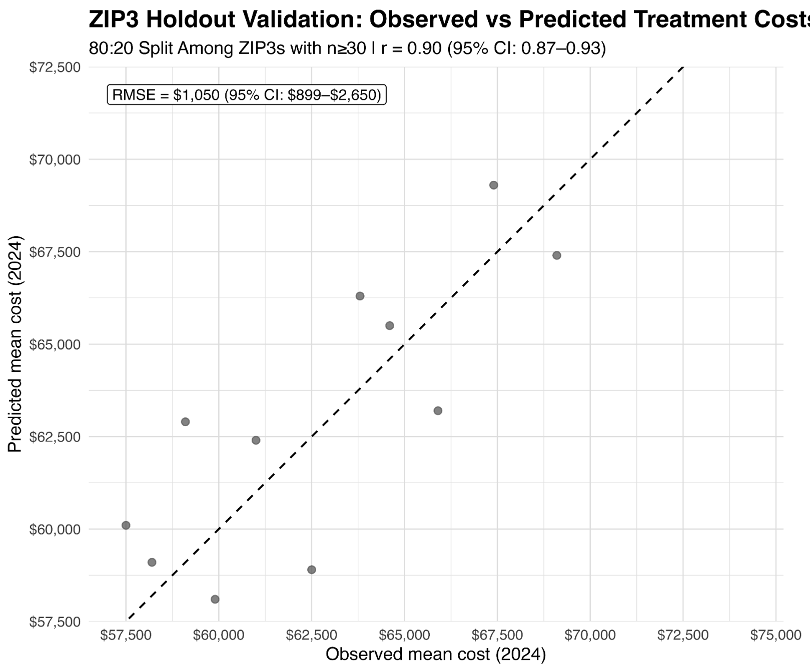

Geographic Structure of County Treatment Costs

Before smoothing, county-level treatment costs were highly dispersed. The mean raw county cost was \$68,540 per treated patient (median, \$66,722; interquartile range, \$57,374–\$76,670), and annual county P90/P10 ratios ranged from 2.3 to 3.4. Moran's I was 0.583 ($P < .001$), indicating that counties with similar treatment costs were geographically clustered rather than randomly distributed.[26] The raw county cost distribution is shown in eFigure 2.3 in the Appendix.

After Bayesian spatiotemporal smoothing, stable cost predictions were available for all US counties (Figure 2.2). The case-weighted national mean predicted 30-day treatment cost was $67,275 per treated firearm-injury patient; the corresponding case-weighted county distribution had a median of $66,985 (interquartile range, $64,340–$70,525). Across counties, the unweighted mean predicted cost was $67,682 per treated patient, with a median of $67,521 and an interquartile range of $62,811–$71,893. The case-weighted estimate is interpreted as the national point estimate, whereas the county distribution describes geographic variation in expected treatment costs across local areas.

The estimated distance over which predicted costs remained spatially correlated was **222 km** (95% credible interval, 197–250 km), indicating that treatment-cost patterns were regionally organized rather than randomly distributed across counties. Figure 2.3 shows the geographic distribution of prediction uncertainty; the comparison of observed and smoothed cost distributions is shown in eFigure 2.4 in the Appendix. Prediction uncertainty was highest in data-sparse regions and in selected large urban counties, including Los Angeles and Miami-Dade. The magnitude of the 30-day estimates was broadly consistent with hospitalization-based payment estimates reported in prior firearm injury cost studies, while reflecting a broader episode of care than index hospitalization alone.[18,20]

Figure 2.2. Spatially smoothed county-specific predicted mean 30-day treatment cost per treated firearm injury patient, United States, 2016–2024 (2024 USD).

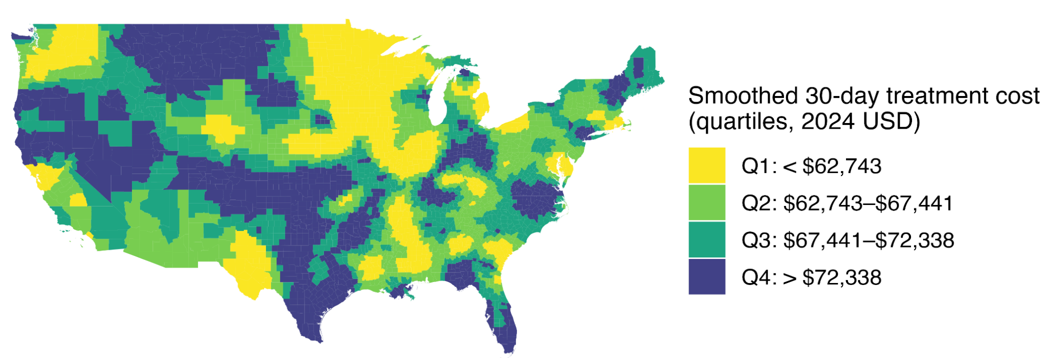

Figure 2.3. Posterior standard deviation of predicted county-level costs. Higher values indicate greater reliance on spatial borrowing.

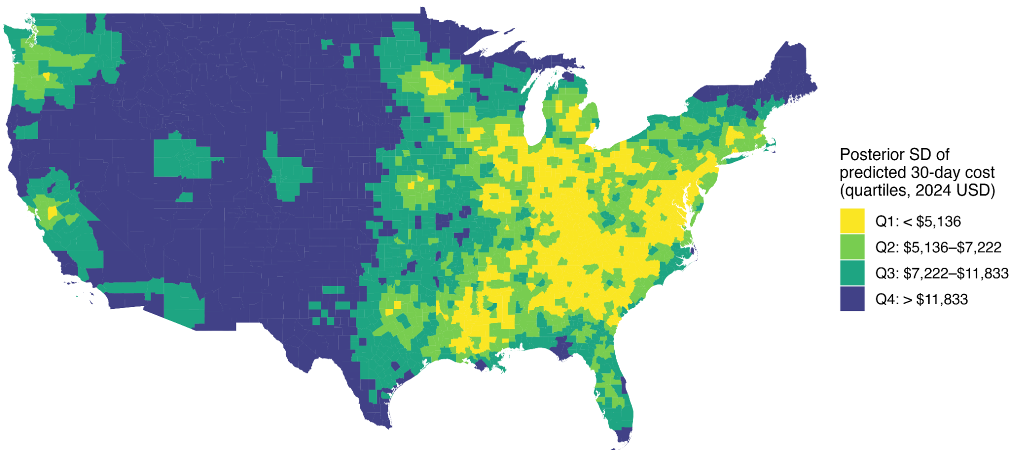

Sequential Decomposition of Geographic Cost Variation

In the as-observed prediction surfaces, the mean annual county P90/P10 ratio was 1.86 in the baseline model (Table 2.2). Adjustment for local Medicare reimbursement geography produced the largest single-step reduction, lowering the ratio to 1.69. Adding payer mix and insurance-market structure further reduced the ratio to 1.59, indicating that local financing conditions were associated with additional geographic dispersion beyond Medicare payment geography. Subsequent adjustment for demographic composition, injury burden, deprivation, local violence burden, health care capacity, and regional utilization norms reduced the ratio to 1.51 in the fully adjusted model. In the standardized prediction surfaces, the corresponding ratio declined from 1.85 at baseline to 1.68 after payment adjustment and to 1.50 in the fully adjusted model. Thus, even after full adjustment, counties near the top of the predicted cost distribution had costs approximately 51% higher than counties near the bottom.

Table 2.2. Mean Annual County P90/P10 Ratios Across Sequential Models, 2016–2024.

Model	P90/P10 (As Obs.)	P90/P10 (Std.)	WAIC	Interpretation
1	**1.86 (1.70–2.15)**	**1.85 (1.69–2.15)**	**355,538**	**Baseline geographic inequality; reference specification**
2	1.69 (1.59–1.81)	1.68 (1.57–1.80)	304,236	Geographic inequality after adjustment for local reimbursement geography
3	1.59 (1.51–1.80)	1.57 (1.51–1.79)	299,320	Geographic inequality after additional adjustment for payer mix and insurance-market structure
4	1.58 (1.50–1.80)	1.56 (1.50–1.79)	298,050	Geographic inequality after additional adjustment for demographic composition
5	1.54 (1.49–1.77)	1.53 (1.45–1.76)	295,725	Geographic inequality after additional adjustment for injury burden, deprivation, and local violence burden
6	1.53 (1.47–1.76)	1.52 (1.44–1.75)	294,290	Geographic inequality after additional adjustment for health care capacity
7	**1.51 (1.42–1.73)**	**1.50 (1.41–1.72)**	**292,110**	**Fully adjusted; geographic inequality after additional adjustment for regional utilization norms**

Notes. P90/P10 values are means of the annual county-level ratios across 2016–2024. Parenthetical values are the annual minimum and maximum. WAIC: lower values indicate better relative fit. Model attenuation is interpreted descriptively as the degree to which each contextual domain is associated with geographic inequality in predicted costs, not as the causal contribution of that domain.

Thirty-Day Mortality

Thirty-day mortality was 1.1% (112 of 10,343 treated patients) and was estimable in only 154 counties. Geographic variation in mortality was limited relative to the variation in treatment costs; the county-level mortality map is shown in eFigure 2.5 in the Appendix.

Discussion

In this national analysis of treated firearm injuries, the case-weighted national mean predicted 30-day treatment cost was $67,275 per treated patient. County-level costs were regionally organized, and adjustment for local Medicare reimbursement geography produced the largest single-step reduction in geographic inequality, with the mean annual county-level P90/P10 declining from 1.86 to 1.69. Adding payer mix and insurance-market structure further reduced the ratio to 1.59, suggesting that local financing conditions account for variation beyond Medicare payment geography alone. The reduction was incomplete. After further adjustment for demographic composition, injury burden, deprivation, local violence burden, health care capacity, and regional utilization norms, the mean annual P90/P10 remained 1.51, leaving counties near the top of the distribution with predicted costs approximately 51% higher than counties near the bottom.

This pattern is consistent with prior work showing that geographic price adjustment narrows regional spending differences without eliminating them.[10] In our setting, payment geography and payer-market structure both mattered, but neither accounted for the residual spatial pattern. That pattern remained strongly regional: the estimated spatial correlation range of 222 km aligns more closely with hospital market areas and trauma referral networks than with county-level decision-making, suggesting that regional delivery-system organization is a plausible contributor to persistent cost clustering.[25]

Elevated posterior uncertainty in some large urban counties, including Los Angeles and Miami-Dade, likely reflects within-county heterogeneity rather than data sparsity. These counties aggregate multiple trauma centers, neighborhood-level severity gradients, payer-mix differences, referral patterns, and distinct treatment pathways into a single county mean — a level of internal complexity that a county-level estimate cannot resolve. This is consistent with evidence that high-spending urban regions can remain variable after price adjustment because utilization patterns and local delivery-system structure differ in ways that measured reimbursement geography does not capture.[10]

These findings have several policy implications. For trauma-system planning, the estimated spatial correlation range suggests that regional coordination may be more consequential than county-level planning alone. For CMS and state Medicaid programs, the county cost surface provides a basis for evaluating whether existing geographic payment adjusters align with empirically observed treatment-cost patterns for high-acuity trauma episodes. For surveillance, the uncertainty estimates identify counties where measurement depends most heavily on spatial borrowing and where linkage of claims, trauma registry, and emergency department data could most improve local precision. These findings should be interpreted as a descriptive baseline, not as evidence of inefficiency or inappropriate practice.

Limitations

Several limitations should be considered. First, the cohort was restricted to patients who survived to receive emergency department or inpatient care and had sufficiently stable insurance enrollment for 30-day episode construction, excluding those who died before reaching a facility and those with intermittent or absent coverage. Second, inverse-probability weighting improved comparability on observed demographic characteristics but cannot eliminate selection on unobserved factors associated with both coverage and spending. Third, injury severity, frailty, and broader case mix were not directly measured, so residual geographic inequality may partly reflect unmeasured differences in clinical need rather than differences in care delivery. Fourth, several covariates were proxies measured on geographic units that required crosswalk translation; although sensitivity analyses did not alter the core findings, residual measurement error likely attenuated the estimated contribution of measured covariates. Finally, county-level estimates in dense urban areas may mask substantial within-county heterogeneity in injury severity, referral patterns, payer mix, and treatment pathways — a limitation that finer-grained data linkage would be best positioned to address.

Conclusion

Firearm injury treatment costs are strongly regionally organized across US counties and display geographic inequality that persists after accounting for local Medicare reimbursement geography, payer-market structure, and measured demographic, contextual, and health care system factors. Payment geography explained a meaningful but incomplete share of the observed dispersion. The county-level cost surface produced here provides a new empirical baseline for trauma-system planning, geographic payment calibration, and firearm-injury surveillance. Future studies linking trauma registry data with insurance claims would be best positioned to distinguish regional delivery-system organization from unmeasured clinical need as drivers of the residual geographic inequality.

References

1. Centers for Disease Control and Prevention, National Center for Injury Prevention and Control. Firearm violence prevention. Accessed March 2026. https://www.cdc.gov/violenceprevention/firearms
2. US Government Accountability Office. Firearm Injuries: Health Care Service Needs and Costs. GAO-21-515. Washington, DC: US Government Accountability Office; 2021.
3. Royan R, Lundberg A, Shan Y, Thomas AC, Stey AM. Health care costs of firearm injury hospital visits in the US. *JAMA Health Forum*. 2025;6(9):e253299.
4. Cook A, Osler T, Hosmer D, et al. Gunshot wounds resulting in hospitalization in the United States: 2004–2013. *Injury*. 2017;48(3):621–627.
5. Moscone F, Skinner JS, Tosetti E, Yasaitis LC. The association between medical care utilization and health outcomes: a spatial analysis. *Reg Sci Urban Econ*. 2019;78:103467.
6. Baltagi BH, Moscone F, Santos R. Spatial health econometrics. In: *Health Econometrics*. Emerald Publishing; 2018.
7. Williams AD, Parham MJ, Mercado AE, et al. Geospatial access to trauma care and firearm injury mortality. *J Trauma Acute Care Surg*. Published online January 12, 2026.
8. Wennberg JE. Unwarranted variations in healthcare delivery. *BMJ*. 2002;325(7370):961–964.
9. Fisher ES, Wennberg DE, Stukel TA, et al. Regional variations in Medicare spending, Part 1. *Ann Intern Med*. 2003;138(4):273–287.
10. Gottlieb DJ, Zhou W, Song Y, Andrews KG, Skinner JS, Sutherland JM. Prices don't drive regional Medicare spending variations. *Health Aff*. 2010;29(3):537–543.
11. Finkelstein A, Gentzkow M, Williams H. Sources of geographic variation in health care. *Q J Econ*. 2016;131(4):1681–1726.
12. US Census Bureau. American Community Survey Public Use Microdata Sample (PUMS) documentation. 2023.
13. Missouri Census Data Center. Geocorr 2022: geographic correspondence engine. University of Missouri; 2022.
14. Wilson R, Din A. Understanding and enhancing HUD's ZIP Code Crosswalk Files. *Cityscape*. 2018;20(2):277–294.
15. Dartmouth Atlas of Health Care. Data by geography. The Dartmouth Institute for Health Policy & Clinical Practice.
16. Pulcini CD, Goyal MK, De Souza HG, et al. A firearm violence research methodologic pitfall to avoid. *Acad Emerg Med*. 2022;29(9):1140–1145.
17. Miller GF, Barnett SBL, Florence CS, et al. Costs of fatal and nonfatal firearm injuries in the US, 2019 and 2020. *Am J Prev Med*. 2024;66(2):195–204.
18. Ranney ML, Herges C, Metcalfe L, et al. Increases in actual health care costs and claims after firearm injury. *Ann Intern Med*. 2020;173(12):949–955.

19. Peterson C, Xu L, Florence C. Average medical cost of fatal and non-fatal injuries by type in the USA. *Inj Prev*. 2021;27(1):24–33.
20. Spitzer SA, Staudenmayer KL, Tennakoon L, Spain DA, Weiser TG. Costs and financial burden of initial hospitalizations for firearm injuries, 2006–2014. *Am J Public Health*. 2017;107(5):770–774.
21. US Bureau of Labor Statistics. Consumer Price Index for All Urban Consumers: medical care. 2024.
22. Basu A, Manning WG. Estimating lifetime or episode-of-illness costs under censoring. *Health Econ*. 2010;19(9):1010–1028.
23. Lindgren F, Rue H, Lindström J. An explicit link between Gaussian fields and Gaussian Markov random fields: the SPDE approach. *J R Stat Soc Series B*. 2011;73(4):423–498.
24. Rue H, Martino S, Chopin N. Approximate Bayesian inference for latent Gaussian models using INLA. *J R Stat Soc Series B*. 2009;71(2):319–392.
25. Branas CC, MacKenzie EJ, Williams JC, et al. Access to trauma centers in the United States. *JAMA*. 2005;293(21):2626–2633.
26. Moran PAP. Notes on continuous stochastic phenomena. *Biometrika*. 1950;37(1–2):17–23.

Chapter 2 Appendix

Supplemental Tables, Figures, and Methods

---

eTable 2.1. Covariates Used in Sequential Spatial Models.

Variable	Source	Geography	Years	Operational definition	Concept proxied
Model 2 (local Medicare reimbursement geography)					
Hospital wage index	CMS IPPS Wage Index	Hospital→county →ZIP3	2016–2024	Annual ZIP3-level CMS hospital wage index, aggregated from hospitals to counties and fractionally allocated	Local hospital reimbursement environment
Physician practice expense GPCI	CMS Physician Fee Schedule GPCI	Locality→county →ZIP3	2016–2024	Annual ZIP3-level physician practice expense GPCI, linked from CMS localities and fractionally allocated	Local physician reimbursement environment
Model 3 (payer mix and insurance-market structure)					
Medicaid share	ACS PUMS (ZIP5→PUMA →ZIP3)	ZIP3	2016–2024	Proportion covered by Medicaid	Public-payer mix
Commercial insurance share	ACS PUMS	ZIP3	2016–2024	Proportion covered by employer-sponsored or direct-purchase private insurance	Commercial-payer mix
Uninsured share	ACS PUMS	ZIP3	2016–2024	Proportion uninsured	Uncompensated-care burden
Medicare Advantage HHI	CMS Medicare Advantage enrollment files	County → ZIP3	2016–2024	Herfindahl–Hirschman Index of Medicare Advantage enrollment shares across parent organizations	Local insurance-market concentration
Model 4 (demographic composition)					
Male population share	ACS PUMS (ZIP5→PUMA →ZIP3)	ZIP3	2016–2024	Proportion of ZIP3 population that is male	Local sex composition
Age 18–34 share	ACS PUMS	ZIP3	2016–2024	Proportion aged 18–34	Younger adult age structure
Age 35–49 share	ACS PUMS	ZIP3	2016–2024	Proportion aged 35–49	Mid-adult age structure
Age 50–64 share	ACS PUMS	ZIP3	2016–2024	Proportion aged 50–64	Older working-age structure
Age 65+ share	ACS PUMS	ZIP3	2016–2024	Proportion aged 65+	Older adult structure

Variable	Source	Geography	Years	Operational definition	Concept proxied
Model 5 (injury burden, deprivation, and local violence burden)					
Injury death rate	CHR	County	2016–2024	Annual county injury death rate	General injury burden
Drug overdose death rate	CHR	County	2016–2024	Annual county drug overdose death rate	Substance-use burden
Poverty rate	CHR	County	2016–2024	% residents below federal poverty line	Socioeconomic deprivation
Unemployment rate	CHR	County	2016–2024	County unemployment rate	Local economic distress
Severe housing problems	CHR	County	2016–2024	% households with severe housing problems	Housing instability
Homicide rate	CHR	County	2016–2024	Annual county homicide rate	Local violence burden / violent-injury exposure
Model 6 (health care capacity)					
Hospital beds per 1,000	Dartmouth Atlas	HRR/HSA	Cross-sectional	Hospital beds per 1,000 residents	Inpatient capacity
Registered nurses per 1,000	Dartmouth Atlas	HRR/HSA	Cross-sectional	RNs per 1,000 residents	Nursing workforce capacity
Surgeons per 100,000	Dartmouth Atlas	HRR/HSA	Cross-sectional	Surgeons per 100,000 residents	Surgical capacity
Emergency physicians per 100,000	Dartmouth Atlas	HRR/HSA	Cross-sectional	EM physicians per 100,000 residents	Acute care staffing
Critical care physicians per 100,000	Dartmouth Atlas	HRR/HSA	Cross-sectional	Critical care physicians per 100,000 residents	ICU-level capacity
Model 7 (utilization norms)					
Ambulatory care–sensitive discharges per 1,000	Dartmouth Atlas	HRR/HSA	Cross-sectional	ACS discharges per 1,000 residents	Access-sensitive utilization norm
Medical discharges per 1,000	Dartmouth Atlas	HRR/HSA	Cross-sectional	Medical discharges per 1,000 residents	General admission tendency
Surgical discharges per 1,000	Dartmouth Atlas	HRR/HSA	Cross-sectional	Surgical discharges per 1,000 residents	Procedure intensity

Notes. ACS covariates were constructed at the ZIP3 level by harmonizing PUMA-level ACS microdata using population-weighted ZIP5-to-PUMA crosswalks. Dartmouth Atlas variables were measured in service-market geographies and translated to ZIP3 using ZIP-based crosswalks. CHR = County Health Rankings; CMS = Centers for Medicare & Medicaid Services; GPCI = Geographic Practice Cost Index; HHI = Herfindahl–Hirschman Index; HRR = hospital referral region; HSA = hospital service area; IPPS = Inpatient Prospective Payment System; PUMS = Public Use Microdata Sample; ZIP3 = 3-digit ZIP code prefix. All covariates are interpreted as contextual proxies for hypothesized sources of geographic variation in paid 30-day treatment costs, rather than as causal mediators or confounders in a single pathway.

eTable 2.2. Study Population, Follow-Up, and Geographic Coverage.

Metric	Value
Study period	2016–2024
Eligible patients identified	12,928
Excluded (insufficient enrollment)	2,585
Final analytic cohort	10,343
Administrative censoring	0.56%
30-day mortality	112 (1.1%)
—	
Total ZIP3 regions	897
ZIP3s with ≥1 encounter	85% (n = 760)
ZIP3s with ≥10 encounters	30% (n = 269)
Population covered	~98% (~323.5M)
Counties represented	3,023 of 3,235 (93.4%)

Notes. Patients were required to have at least 180 days of pre-index enrollment and active coverage on the index date. All individuals were followed for up to 30 days, and costs accrued through the date of death were fully observed. Although geographic coverage was broad, only 30% of ZIP3s had at least 10 encounters during the study period, indicating substantial sparsity in the raw local inputs and motivating the stricter threshold of **n ≥ 30** used for holdout validation (Section 4.3).

eTable 2.3. Sensitivity Analysis Results for Primary Spatial Model Outputs, 2016–2024.

Specification	Details	P90/P10 M1 (AO)	P90/P10 M7 (AO)	P90/P10 M7 (Std.)	Range (km)	Holdout correlation
Reference	PC priors [P(ρ<300km)=0.5; P(σ>1)=0.01]; HUD 2022; annual CHR; Dartmouth 2019	**1.86**	**1.51**	**1.50**	**222**	**0.90**
Tighter range prior	P(range<200km)=0.5	1.87	1.52	1.51	209	0.89
Looser range prior	P(range<400km)=0.5	1.86	1.51	1.50	234	0.89
Finer mesh	Max edge length −25%	1.86	1.51	1.50	224	0.89
Coarser mesh	Max edge length +25%	1.87	1.52	1.51	219	0.89
Independent annual fields	No AR(1) structure	1.88	1.53	1.52	218	0.88
HUD crosswalk 2018	2018 vintage	1.86	1.51	1.50	222	0.89
Hard county assignment	No fractional allocation	1.89	1.54	1.53	220	0.88
Payment geography excluded	Full model excluding payment geography	1.86	1.68	1.66	211	0.89
Block order permuted	Injury burden before demographics	1.86	1.51	1.50	222	0.89

Notes. AO = as-observed; Std. = standardized; PC = penalized complexity. The reference specification used PC priors $P(range < 300\ km) = 0.5$ and $P(\sigma > 1) = 0.01$, the 2022 HUD crosswalk, annual County Health Rankings measures, and Dartmouth Atlas 2019 capacity and utilization measures. Holdout correlation compares predicted and observed costs in held-out ZIP3-year cells. Moran's I was calculated using smoothed county-level predicted costs. Across sensitivity specifications, treatment costs remained strongly spatially clustered, the estimated spatial range remained regional in scale, and geographic dispersion declined after full adjustment but remained substantial. Excluding Medicare payment geography produced the largest change in the fully adjusted P90/P10 ratio, increasing it from 1.51 to 1.68.

eFigure 2.1. County-level firearm-injury encounter rates per 100,000 population, United States, 2016–2024.

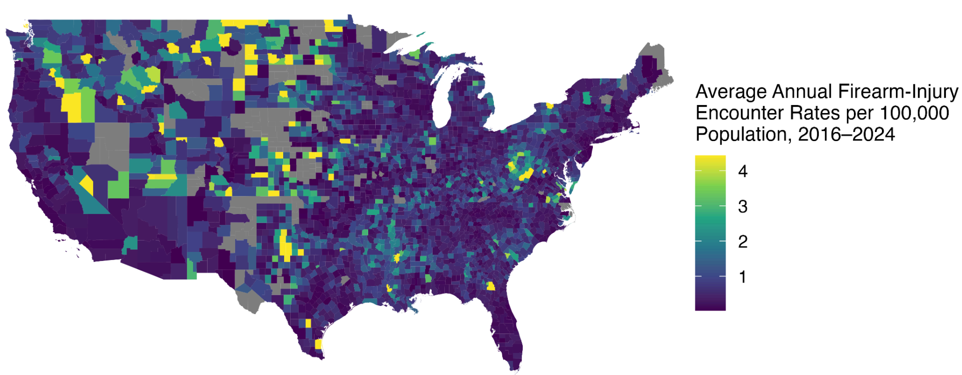

eFigure 2.2. Distribution of ZIP3 case volume used to construct local treatment-cost inputs, United States, 2016–2024.

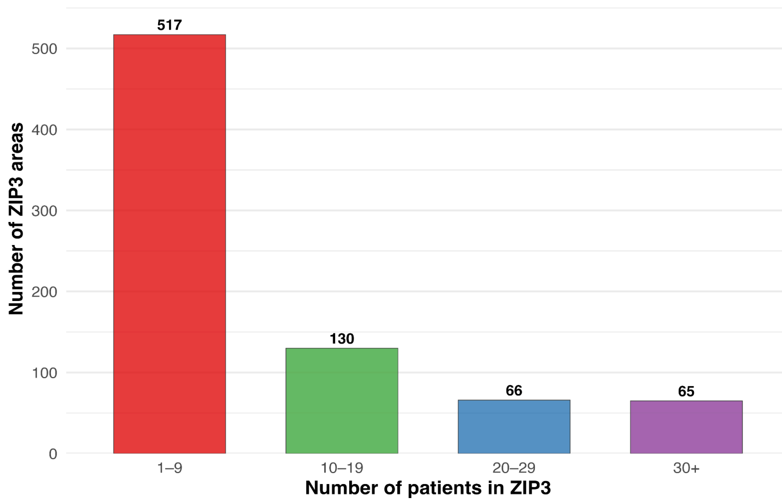

eFigure 2.3. Distribution of county-level mean 30-day treatment cost per treated firearm injury patient (2024 USD), prior to spatial smoothing.

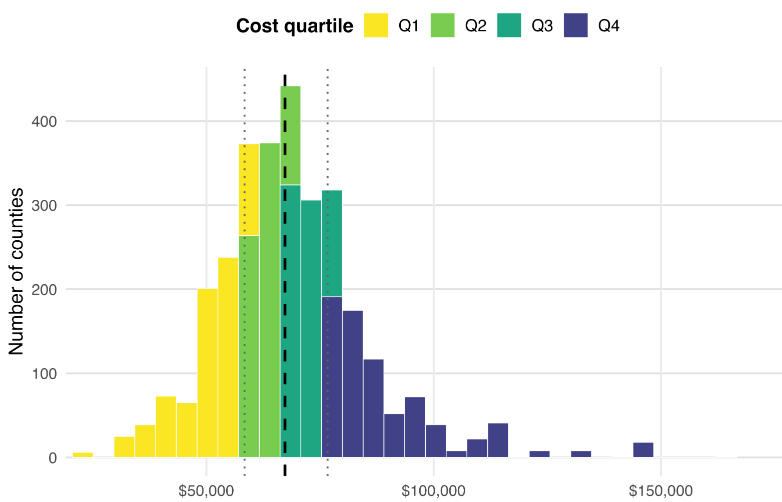

eFigure 2.4. Distribution of observed and spatially smoothed county-level mean 30-day treatment costs.

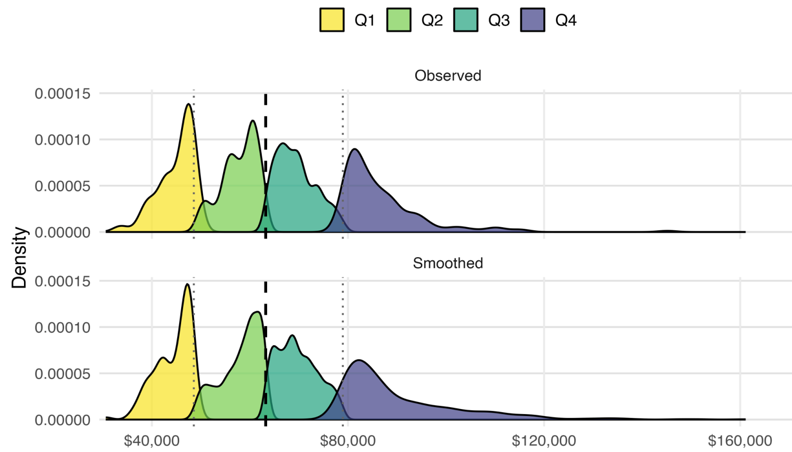

eFigure 2.5. County-level 30-day mortality following firearm injury, United States, 2016–2024.

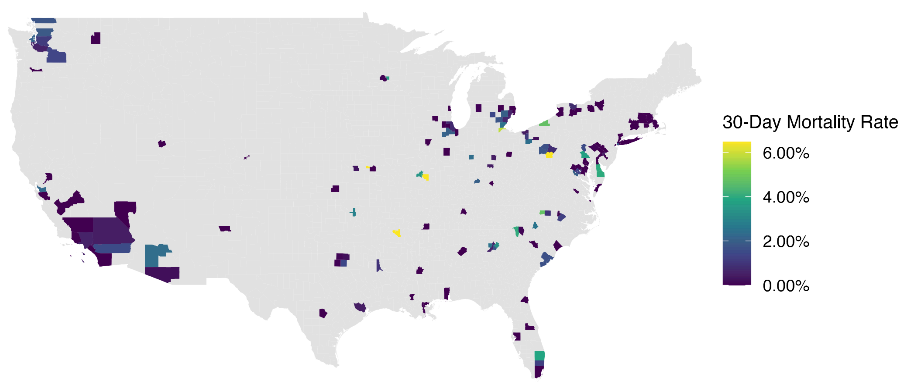

eFigure 2.6. ZIP3-level mean 30-day firearm-injury treatment costs by case-volume stratum, United States, 2016–2024 (2024 USD).

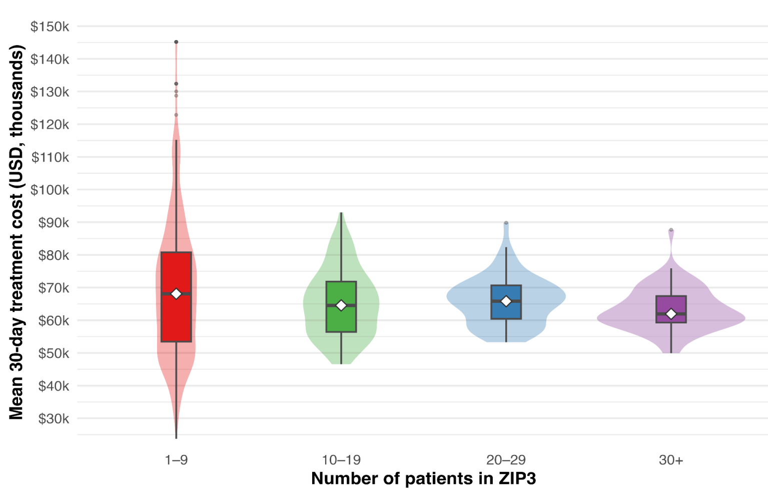

eFigure 2.7. Distribution of spatially smoothed county-specific predicted mean 30-day treatment cost per treated firearm-injury patient, United States, 2016–2024 (2024 USD): unweighted and case-weighted county distributions.

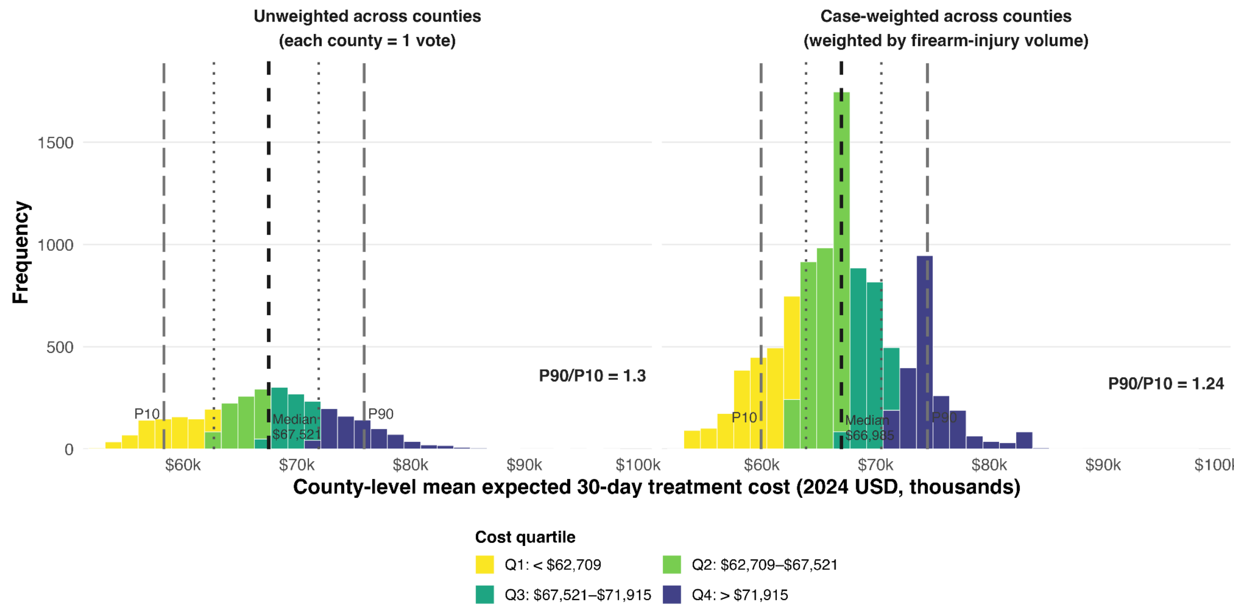

eMethods 1. Geographic Harmonization Across Data Sources

The analysis combined data sources reported on different geographic units. Komodo claims identify beneficiary residence at the 3-digit ZIP code level (ZIP3), ACS microdata are released at the Public Use Microdata Area (PUMA) level, County Health Rankings (CHR) measures are reported at the county-year level, Dartmouth Atlas measures are reported for Hospital Service Areas (HSAs) and Hospital Referral Regions (HRRs), and CMS payment files are defined using county-, Core-Based Statistical Areas (CBSA)-, or payment-locality-based structures. Geographic harmonization was therefore required before population calibration, covariate linkage, and county-level prediction.

ZIP5 areas served as the common bridging geography. ZIP5-to-PUMA, ZIP5-to-county, and ZIP5-to-service-area crosswalks were used to translate each source into a common ZIP3- or county-level frame. In each step, translation used residential population-weighted fractional shares rather than deterministic assignment.

ACS to ZIP3

ACS microdata were used only to construct demographic benchmarks for inverse-probability weighting. Because ACS records are released at the PUMA level without ZIP identifiers, we used the Missouri Census Data Center Geocorr correspondence engine to link ZIP5 areas to PUMAs. For each ZIP3, ZIP5-to-PUMA fractional shares were aggregated using ZIP5 population weights to produce ZIP3-specific PUMA weights summing to 1:

$$X_z = \sum_p \omega_{zp} X_p$$

where X_z is the ZIP3-level benchmark quantity, X_p is the corresponding PUMA-level ACS quantity, and ω_{zp} is the population-weighted share of ZIP3 z residing in PUMA p. This procedure was applied to each demographic cell used in the weighting model.

CHR, Dartmouth Atlas, and CMS to ZIP3

CHR variables were translated from county-year to ZIP3-year values using population-weighted ZIP5-to-county shares aggregated to ZIP3. Dartmouth Atlas measures were linked from HSA/HRR to ZIP5 using the Dartmouth crosswalk and aggregated to ZIP3 using ZIP5 population weights. CMS Hospital Wage Index values were translated from provider/payment geography files to counties and then to ZIP3. Physician GPCIs were linked from CMS payment localities to counties and then translated to ZIP3. All CMS payment variables were treated as contextual proxies rather than patient-level payment rates.

ZIP3-to-county allocation of predicted costs

The spatial model was estimated at the ZIP3-year level. ZIP3-level posterior mean predicted costs were then allocated to counties using fractional ZIP3-to-county population shares derived from the HUD ZIP5-to-county crosswalk:

$$\widehat{C}_{ct} = \sum_z a_{zc} \widehat{C}_{zt}$$

where $\widehat{C}_{zt}$ is the ZIP3-year posterior mean predicted cost and a_{zc} is the share of the ZIP3 population residing in county c, with $\sum_c a_{zc} = 1$ for each ZIP3. This approach preserves geographic continuity and avoids the discontinuities introduced by hard ZIP3-to-county assignment.

Sensitivity checks

Sensitivity analyses using alternative crosswalk vintages (HUD 2018, HUD 2020) and deterministic hard assignment produced substantively similar results (eTable 3). Hard assignment increased the fully adjusted P90/P10 from 1.61 to 1.64 and reduced holdout ρ from 0.894 to 0.881, consistent with the expected effect of imposing artificial county boundaries on a spatially continuous surface.

eMethods 2. Spatial Model Specification: Mesh Construction, Priors, and Temporal Structure

---

ZIP3-level expected 30-day treatment costs were modeled as a continuous spatiotemporal process using the stochastic partial differential equation (SPDE) representation of a Matérn Gaussian field, estimated with Integrated Nested Laplace Approximation (INLA). This approach provides stable small-area estimates, explicit posterior uncertainty, and spatial borrowing across nearby ZIP3 areas and adjacent years.

Spatial unit and projection

The analytic unit for modeling was the ZIP3 centroid-year. All spatial operations were performed in the contiguous US Albers equal-area projection (EPSG:5070). Reported distances, including the posterior spatial range, are expressed in kilometers.

Mesh construction

The SPDE mesh was constructed as a constrained Delaunay triangulation over the continental United States using ZIP3 centroid locations. A nonconvex hull was fit around the observed centroids and extended with an outer buffer to reduce boundary artifacts. Mesh density was finer in ZIP3-dense regions and coarser in sparse regions. The same mesh was used across all sequential models to preserve comparability of the latent spatial field.

Outcome model

Let Y_{zt} denote the ZIP3-year weighted mean expected 30-day treatment cost per treated patient after inverse-probability weighting and Kaplan-Meier sample average estimation. Conditional on the latent field and included covariates, Y_{zt} was modeled with a Gaussian likelihood. The baseline model was

$$Y_{zt} = \beta_0 + s(z,t) + \epsilon_{zt}$$

where $s(z,t)$ is the latent spatiotemporal field and ϵ_{zt} is an exchangeable Gaussian residual.

Sequentially adjusted models added covariate blocks while retaining the same spatial and temporal structure:

$$C_{z,t} = \beta_0 + P_{z,t}\Gamma_P + D_{z,t}\Gamma_D + R_{z,t}\Gamma_R + H_{z,t}\Gamma_H + U_{z,t}\Gamma_U + s(z,t) + \epsilon_{z,t}$$

where $P_{z,t}$ denotes local Medicare reimbursement geography, $D_{z,t}$ demographic composition, $R_{z,t}$ injury burden and deprivation, $H_{z,t}$ health care capacity, and $U_{z,t}$ utilization norms. Only the covariate set changed across Models 1 through 6; the mesh, priors, and temporal structure were held fixed.

Penalized-complexity priors

PC priors were placed on the Matérn range and marginal standard deviation parameters: $P(\rho < 300 \text{ km}) = 0.5$ and $P(\sigma > 1) = 0.01$. These priors regularize against overly local or highly variable spatial surfaces. Fixed effects were assigned weakly informative default priors in INLA. Sensitivity analyses using alternative prior settings are summarized in eTable 3.

Temporal structure

Temporal variation was modeled in two parts: a fixed year effect to capture the national secular trend and year-specific spatial deviations modeled with a first-order autoregressive [AR(1)] structure. Alternative temporal specifications (independent annual fields, first-order random walk) were examined in sensitivity analyses and did not materially change the spatial range or inequality summaries.

Model fit and validation

Model fit was assessed using WAIC (lower = better). WAIC values for all six models are reported in Table 2. Interpolation performance was evaluated using an 80/20 holdout design restricted to ZIP3 areas with at least 30 observed patients. Agreement between predicted and observed ZIP3 mean costs was assessed using the Pearson correlation and RMSE.

Supplement 2

Data Processing and Cohort Construction

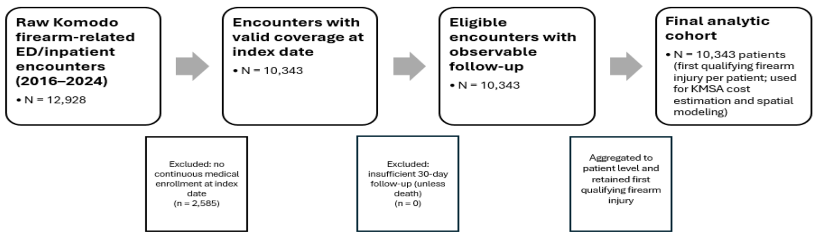

Firearm injury case definition

Firearm injuries were identified using ICD-10-CM external cause-of-injury codes corresponding to powder-fired weapons. Consistent with Pulcini et al., (**28**) we excluded codes corresponding to non-powder firearms (e.g., air guns, BB guns, paintball guns), which are embedded within commonly used firearm code ranges but are epidemiologically distinct and not associated with fatal firearm injury. The full list of included and excluded ICD-10-CM codes is provided in Table A2. This approach aligns with CDC WISQARS definitions for non-fatal firearm injury surveillance.

eTable 2.5: ICD-10-CM Codes Used to Identify Firearm Injuries

Injury intent	ICD-10-CM code range	Description	Included	Rationale
Unintentional	W32.0–W32.9; W33.0–W33.9; W34.00; W34.09	Accidental discharge of handgun or larger powder-fired firearm	Yes	Consistent with CDC WISQARS and firearm injury surveillance definitions
Unintentional	W34.01; W34.11; W34.18	Accidental discharge involving airgun, paintball, or gas-operated gun	No	Non-powder firearm; excluded per Pulcini et al.
Assault	X93.0–X93.9; X94.0–X94.9; X95.0–X95.9	Assault by powder-fired handgun, shotgun, rifle, or unspecified firearm	Yes	Represents assault-related civilian firearm injury.

Assault	X95.01; X95.02; X95.09	Assault involving airgun or paintball gun	No	Non-powder firearm mechanism
Self-harm	X72.0–X72.9; X73.0–X73.9; X74.0–X74.9	Intentional self-harm by powder-fired firearm	Yes	Represents intentional self-inflicted firearm injury
Self-harm	X74.01; X74.02; X74.09	Self-harm involving airgun or paintball gun	No	Non-powder firearm mechanism
Undetermined	Y22.0–Y22.9; Y23.0–Y23.9; Y24.8–Y24.9	Firearm discharge of undetermined intent (powder-fired)	Yes	Included to preserve standard surveillance definitions for powder-fired firearm injury when intent is unknown.
Undetermined	Y24.0	Undetermined discharge involving airgun	No	Non-powder firearm mechanism
Legal / War / Terrorism	Y35–Y38	Firearm injury due to legal intervention, war, or terrorism	No	Excluded to focus on civilian firearm injuries

Notes:

ICD-10-CM codes correspond to external cause-of-injury codes for firearm-related trauma.

Non-powder firearms (air guns, BB guns, paintball guns, and gas-operated guns) were excluded.

All initial, subsequent, and sequela encounter extensions (A, D, S) were retained.

Case definition follows recommendations in Pulcini et al. (2022) and CDC WISQARS.

eTable 2.6: Population Balance Before and After IPW

Number of cells	Mean |SD| (Pre)	Mean |SD| (Post)	Max |SD| (Pre)	Max |SD| (Post)	Frac |SD| > 0.10 (Post)	ESS/N 10,326/10,331
36,828	0.006	0.006	0.18	0.08	0.0003	0.99

Notes: Absolute standardized differences compare Komodo and ACS proportions across joint ZIP3 × age × sex × insurance strata.

Chapter 3

Drug Prices and Firearm Homicide in High-Exposure U.S. Cities

A Panel Instrumental Variables Study

Ronald Dickerson, MA, MPH, Jing Li, PhD, Ali Rowhani-Rahbar, MD, PhD, Anirban Basu, PhD

Abstract

Importance. Illicit drug prices are a plausible upstream determinant of firearm homicide in U.S. cities, but the direction of the relationship is theoretically ambiguous. Supply-side disruptions that raise prices could intensify market conflict and increase violence, or reduce market activity and decrease violence. Credible estimation has been limited by price endogeneity, sparse transaction data, and potential spatial dependence across cities.

Objective. To estimate whether exogenous changes in illicit drug prices are associated with firearm homicide in high-exposure U.S. cities during the 2016–2023 fentanyl restructuring era.

Design, Setting, and Sample. Panel instrumental variables study of six U.S. cities within 400 miles of a major U.S.–Mexico port of entry: Dallas, Houston, Los Angeles, Phoenix, San Antonio, and San Diego. Cities were observed annually from 2016 through 2023, yielding 48 city-year observations.

Exposure. Integrated, opioid, and stimulant drug-price indices recovered from sparse DEA STRIDE transaction data using drug-specific Bayesian spatiotemporal models with explicit instrument separation. Log drug seizure volume served as the excluded supply-side instrument.

Main Outcome. Annual firearm homicide rate per 100,000 residents.

Results. First-stage coefficients were positive across all three drug-price indices, with F-statistics of 520.3, 39.0, and 27.8 for the integrated, opioid, and stimulant specifications, respectively. Placebo and falsification tests using the same IV structure as the main analysis showed no association between the instrumented integrated drug-price index and officers per capita, homicide clearance rate, lagged firearm homicide, or fatal crash rate. In the primary panel two-stage least squares specifications, estimated effects were negative across all three indices: −1.676 (95% CI, −3.075 to −0.277) for the integrated index, −0.676 (95% CI, −1.834 to 0.482) for the opioid index, and −2.848 (95% CI, −4.071 to −1.625) for the stimulant index. The stimulant estimate was the most precise and excluded zero. Spatial robustness checks produced negative point estimates of similar magnitude after adding spatiotemporal random effects.

Conclusions and Relevance. In six high-exposure U.S. cities from 2016 through 2023, instrumented drug prices were not associated with higher firearm homicide. Point estimates were consistently negative, with the strongest evidence for stimulant prices. These findings are more consistent with a market-contraction mechanism than with a dominant market-conflict mechanism and do not support the assumption that supply-side disruption necessarily increases urban firearm violence. Results should be interpreted cautiously given the small analytic panel, reliance on modeled price recovery from sparse transaction data, annual time scale, and restriction to high-exposure cities near major entry corridors.

Keywords: firearm homicide; illicit drug markets; instrumental variables; supply shocks; spatial econometrics; INLA-SPDE; panel fixed effects; drug prices

I. Introduction

Background

Firearm homicide remains a major public health problem in the United States. In 2023, 17,927 Americans died from firearm homicide, with the burden falling disproportionately on young men in low-income urban communities of color.[1,2] Each fatal injury imposes roughly $10–11 million in lost productivity and quality of life, placing the annual societal burden above $175 billion.[3] Despite sustained policy attention, the upstream structural conditions that shape lethal firearm violence remain incompletely understood.

Illicit drug markets are one plausible upstream factor. Drug market activity is consistently linked to urban violence, and disputes over territory, debt, and supply control are frequently cited in accounts of shootings in large U.S. cities.[4,5] The question has become more salient in the synthetic opioid era. Since roughly 2016, fentanyl, counterfeit pills, and multi-product trafficking networks have reshaped U.S. illicit markets, producing supply chains that are more integrated, more geographically diffuse, and potentially more sensitive to upstream disruption than in earlier periods.[6–9] Yet one causal question remains unsettled: do exogenous changes in local illicit drug-market conditions affect firearm homicide?

This question is distinct from asking whether drug use, drug arrests, or neighborhood drug activity correlate with violence. The focus here is market-level: scarcity, competitive pressure, and illicit drug prices. Upstream disruptions could raise violence by destabilizing markets and intensifying organizational conflict, or reduce violence by contracting illicit activity and the number of contested transactions. The direction is therefore an empirical question.

Conceptual mechanism

Goldstein's tripartite framework identifies three channels through which drug markets and violence may be linked: psychopharmacological, economic-compulsive, and systemic.[5] Firearm homicide is most closely tied to the systemic channel, which concerns violence arising from territorial competition, debt enforcement, and organizational coercion in markets that lack legal dispute resolution. By contrast, the economic-compulsive channel is more closely tied to acquisitive offending. Prior price-crime evidence on property crime therefore need not generalize directly to firearm homicide.

Within the systemic channel, two mechanisms can link supply-driven changes in drug prices to firearm homicide, and they point in opposite directions. The first is a *market-conflict mechanism*. Castillo, Mejía, and Restrepo (2018) formalize a setting in which supply disruptions raise prices and, under sufficiently inelastic demand, increase market rents, raise the value of territorial control, and intensify competition among organizations that rely on coercion rather than contracts.[10,11] Castillo et al. estimate that a 10% cocaine supply contraction raised homicide by 2–3% in exposed Mexican municipalities, providing one external benchmark.

The second is a *market-contraction mechanism*. Persistent supply suppression may reduce the volume of illicit market activity itself, producing fewer transactions, fewer disputes, and fewer contested territories. DeSimone (2001), the most recent U.S. study to use a comparable supply-side identification strategy, found that higher cocaine prices were associated with lower property crime and a lower murder rate.[12] The latter finding is directly analogous to the outcome studied here and points in the opposite direction from the conflict-based mechanism.

These mechanisms are not mutually exclusive. Their relative importance likely depends on the time horizon of the shock, the elasticity of demand, and the organizational structure of the affected market. The net effect on firearm homicide therefore cannot be signed a priori. Product-market integration in the synthetic era further complicates the picture: fentanyl has penetrated heroin, stimulant, and counterfeit-pill markets, and shared trafficking corridors connect nominally distinct drug categories.[17–19] This integration motivates an integrated drug price index as the primary exposure, with opioid and stimulant subindices examined as secondary analyses.

Why credible identification remains difficult

Even with a clear conceptual framework, credible estimation faces three linked obstacles. First, *price endogeneity*. Violence, enforcement, and unmeasured market conditions may all affect local prices while also shaping homicide. Because these channels operate simultaneously and in opposing directions, the sign of OLS bias is indeterminate. Second, *measurement noise*. DEA transaction records are not random samples of retail drug prices; they reflect investigative priorities, transaction context, and enforcement patterns.[20–23] In the present panel, only 29% of city-year-drug cells meet the three-transaction minimum for a reliable observed price. Designs conditioned only on observed cells would yield a selective panel biased toward cities with intensive DEA surveillance. Third, *spatial dependence*. Trafficking routes and organizational spillovers cross city boundaries. Osorio (2015) documents that spatial autocorrelation in drug violence rose from 0.10 to 0.58 over a decade in Mexico,[24] and conventional standard errors are anti-conservative when outcomes share geographically correlated shocks.[25,26] No prior U.S. city-panel study has addressed endogeneity, sparse DEA measurement, and spatial dependence in a single design.

Why this matters

The direction of any market-tightening effect is itself policy-relevant. If tightening raises firearm homicide, then some urban gun violence is an unintended downstream cost of interdiction, one not currently incorporated into enforcement cost-benefit frameworks. If tightening reduces firearm homicide, then supply suppression yields a violence-reduction benefit in addition to any overdose effect. If the effect is null at annual frequency, the relevant mechanism may require more concentrated organizational shocks than those visible in city-year data, redirecting future work toward event-based designs. Each outcome carries distinct policy implications. Caulkins (2024) makes the broader point: synthetic-era drug policy should account explicitly for the collateral consequences of interdiction, including violence, rather than assume supply suppression is uniformly beneficial.[27]

Study goals and contributions

This paper estimates whether exogenous changes in illicit drug prices influence firearm homicide in high-exposure U.S. cities from 2016 to 2023. High-exposure cities are defined as those within 400 miles of the nearest U.S.–Mexico port of entry. The primary estimand is the local average treatment effect of a one-standard-deviation increase in the instrumented integrated drug-price index on the log firearm homicide rate, conditional on city fixed effects, year fixed effects, and time-varying controls, for cities whose drug prices respond to the seizure-based instrument. Secondary analyses examine opioid and stimulant drug-price indices separately. Full-sample and alternative-cutoff specifications are reported as sensitivity analyses.

The paper makes four contributions. First, it constructs city-year drug-price measures from sparse DEA transaction data using a drug-specific spatiotemporal recovery step with instrument separation, a design feature that avoids two-step circularity and preserves the interpretability of overidentification tests. Second, it identifies plausibly exogenous variation in drug prices using supply-side seizure shocks in cities with the greatest exposure to major U.S.–Mexico entry corridors. Third, it provides new U.S. city-panel evidence on the drug price–firearm homicide relationship during the 2016–2023 fentanyl restructuring era, with magnitudes directly comparable to earlier studies. Fourth, it evaluates whether spatial structure materially changes inference in this setting.

II. Data

The main analytic sample consists of six high-exposure U.S. cities observed annually from 2016 to 2023. The six cities are San Diego, Los Angeles, Phoenix, San Antonio, Houston, and Dallas. High-exposure cities are defined as those within 400 miles of the nearest U.S.–Mexico port of entry, where seizure-based supply shocks are most informative. Full-sample and alternative-cutoff specifications appear in sensitivity analyses. The 400-mile threshold is not a natural policy boundary. By contrast, the formal La Paz Agreement border region, used by the U.S. Environmental Protection Agency,[34] extends only 100 km from the international boundary and would include only San Diego in this sample. The 400-mile cutoff is instead a substantively motivated threshold that retains cities plausibly exposed to entry-corridor shocks while preserving enough cross-city variation for stable estimation. Table 3.1 summarizes data sources, variables, and analytic roles.

Table 3.1. Data sources, variable definitions, and analytic roles.

Variable	Analytic role	Source	Definition / rationale
A. Outcome			
Firearm homicide rate	Primary outcome	FBI UCR / SHR	Annual firearm homicides per 100,000 residents; city-year measure of lethal firearm violence.
B. Drug-market measures (constructed from DEA STRIDE via Stage 0 recovery)			
Integrated drug-price index	Primary exposure	DEA STRIDE; authors' construction	Equal-weighted mean of standardized recovered prices for cocaine, heroin, fentanyl, and methamphetamine.
Opioid drug-price index	Secondary exposure	DEA STRIDE; authors' construction	Equal-weighted mean of standardized recovered prices for heroin and fentanyl; tests the opioid-market mechanism.
Stimulant drug-price index	Secondary exposure	DEA STRIDE; authors' construction	Equal-weighted mean of standardized recovered prices for cocaine and methamphetamine; tests the stimulant-market mechanism.
Drug-specific recovered price	Index input	DEA STRIDE; Stage 0 recovery	Purity-adjusted price per gram, smoothed through drug-specific spatiotemporal recovery.
C. Excluded instruments (supply-side; not in structural equation)			
Total drug seizure volume	Instrument — integrated model	U.S. CBP	Total seizure volume in pounds at the city-year level; proxies upstream supply disruption.
Opioid seizure volume	Instrument — opioid model	U.S. CBP	Heroin and fentanyl seizure volume in pounds; isolates supply disruption specific to opioid markets.
Stimulant seizure volume	Instrument — stimulant model	U.S. CBP	Cocaine and methamphetamine seizure volume in pounds; isolates supply disruption specific to stimulant markets.
D. Time-varying city-level controls (included in all specifications)			
Total population	Control	ACS / Census	Total city residents; adjusts for city scale and market size.
Unemployment rate	Control	ACS / FRED	Percent of the labor force unemployed; captures local labor-market conditions.
Real per capita income	Control	BEA / FRED	Real per capita personal income; captures local economic opportunity.
Poverty rate	Control	ACS	Percent of residents below the federal poverty line; adjusts for socioeconomic disadvantage.

Variable	Analytic role	Source	Definition / rationale
Demographic composition (% female, % Black, % Hispanic, % married)	Controls	ACS	Population shares adjusting for demographic composition and structural context.
Age composition (% 15–24, % 25–34)	Controls	ACS	Population shares for age groups associated with violence risk.
Educational attainment (% HS, % BA)	Controls	ACS	Adult population aged 18+ with high school or bachelor's degree; proxies human capital.
Officers per capita	Enforcement control; placebo outcome	FBI employment data	Sworn officers per 100,000 residents; absorbs local policing intensity.
Homicide clearance rate	Enforcement control; placebo outcome	FBI UCR	Homicide clearance rate; absorbs enforcement environment.
E. Falsification and placebo outcomes			
Fatal crash rate	Falsification outcome	NHTSA FARS	Fatal motor vehicle crashes per 100,000 residents; outcome without a plausible drug-market mechanism.
Lagged firearm homicide rate	Pre-trend placebo	FBI UCR / SHR	Prior-year firearm homicide rate; tests for correlation with pre-existing violence trends.

Notes: All variables are measured at the city-year level unless otherwise noted. The integrated, opioid, and stimulant drug-price indices are constructed after a Stage 0 spatiotemporal recovery step that fills sparse DEA STRIDE price cells by borrowing information from nearby cities and adjacent years. Seizure measures are excluded from the structural equation and from the Stage 0 recovery formula. ACS = American Community Survey; BEA = Bureau of Economic Analysis; CBP = U.S. Customs and Border Protection; DEA = Drug Enforcement Administration; FARS = Fatality Analysis Reporting System; FBI = Federal Bureau of Investigation; FRED = Federal Reserve Economic Data; SHR = Supplementary Homicide Reports; STRIDE = System to Retrieve Information from Drug Evidence; UCR = Uniform Crime Reports.

Drug price construction

Within each city-year-drug cell, purity-adjusted prices (price per gram divided by purity) are winsorized at the 4th and 86th percentiles of the drug-specific distribution and summarized by the winsorized median. Cells with fewer than three transactions are treated as unreliable. Because sparse or missing cells account for most of the potential city-year-drug grid, and because observed cells overrepresent cities with intensive DEA surveillance, relying only on observed prices would produce a selective panel and discard much of the available information.

Stage 0: spatiotemporal price recovery

To address sparse and selective coverage, Stage 0 estimates drug-specific spatiotemporal models that recover complete city-year price signals from the available transactions. For each substance separately, a Bayesian hierarchical model is fitted using Integrated Nested Laplace Approximation with a Stochastic Partial Differential Equation Matérn spatial field and AR(1) temporal dynamics.[31,32] The spatial component borrows information across nearby cities, while the temporal component links adjacent years. Where price data for one substance are missing in a city-year, observed prices for other substances in the same city-year inform the recovery, reflecting the cross-product integration of contemporary illicit markets. The goal is not to impose a deterministic price surface, but to recover usable city-year signals from highly incomplete transaction data.

A critical design feature is *instrument separation*. Seizure measures and related first-stage variables are excluded from Stage 0 so that the recovered price measure is not partially built from the instruments used later in the IV analysis. This avoids two-step circularity and preserves the interpretation of overidentification tests. Stage 0 performance is evaluated using 20% random holdout cross-validation within drug, with Pearson's r on held-out log-price cells as the primary fit diagnostic.

Drug-price index construction

After Stage 0 recovery, log prices are standardized within drug so that no single substance mechanically dominates the composite. Three equal-weighted city-year drug-price indices are then constructed: an integrated index across all four drugs, an opioid index combining heroin and fentanyl, and a stimulant index combining cocaine and methamphetamine. Equal weighting avoids tying the exposure mechanically to shifts in drug composition. The main analytic sample contains 48 city-year observations (6 cities × 8 years). The broader 224-observation panel (28 cities × 8 years) is retained for the Stage 0 price recovery, which benefits from cross-city information, and for sensitivity specifications reported in the appendix.

III. Empirical Strategy

The empirical strategy has three stages applied to the six-city high-exposure sample. Stage 0 recovers city-year market measures from sparse DEA records, drawing on the full 28-city panel to stabilize the spatial smoothing. Stage 1 tests whether seizure-based supply shocks predict the recovered drug-price indices in the high-exposure sample. Stage 2 estimates the relationship between instrumented drug prices and firearm homicide in the same sample, with spatial robustness checks assessing whether residual geographic structure changes inference.

Identification problem

City-year drug-price measures are potentially endogenous to firearm homicide. Violence may reshape local market organization; enforcement can affect both prices and recorded homicide; and unmeasured city-year conditions may influence both. City and year fixed effects absorb time-invariant city characteristics and common national shocks, but they do not eliminate time-varying simultaneity or omitted-variable bias. Instrumental variable estimation is therefore used to isolate the component of drug-price variation driven by upstream supply shocks.

Stage 1: instrument and first stage

The main excluded instrument is log total drug seizures. The identifying logic is that upstream seizure shocks should be most informative where supply routes from major U.S.–Mexico entry corridors are most relevant. Preliminary full-sample diagnostics showed that the seizure-price relationship is concentrated in cities nearer to entry points and is essentially flat in more distant cities. Restricting the main analysis to high-exposure cities therefore strengthens identification by concentrating the sample where the instrument has structural relevance, and yields a cleaner first stage that no longer requires distance interactions. The first-stage equation is:

$$P_{ct} = \pi_0 + \pi_1 S_{ct} + X_{ct}\varphi + \mu_c + \tau_t + \upsilon_{ct} \qquad (1)$$

where P_{ct} is the drug-price index, S_{ct} is log seizures, X_{ct} is the time-varying control vector, and μ_c and τ_t are city and year fixed effects. Family-specific analyses substitute opioid or stimulant seizure measures for total seizures.

Instrument strength is assessed using two diagnostics. The conventional first-stage F-statistic is reported with the Stock–Yogo threshold of $F > 10$ as a familiar benchmark.[33] Because the conventional F is not robust to heteroskedasticity or clustered errors, the Olea–Pflueger effective F-statistic is also reported as the primary weak-instrument diagnostic in clustered settings.[35] Sensitivity specifications add the purity index as a second excluded instrument, and results are presented both with and without it.

The exclusion restriction requires that seizure shocks affect firearm homicide only through their effect on drug prices, conditional on controls and fixed effects. Three features support this claim within the restricted sample. **First**, enforcement controls — log officers per capita and log clearance rate — absorb the enforcement-climate channel through which seizures might otherwise affect homicide directly. **Second**, the instrument separation in Stage 0 ensures that the excluded instrument is not embedded in the constructed price measure. **Third**, within the high-exposure subsample, residual distance variation is small enough that no port-distance covariate is required in either stage, removing the otherwise subtle mechanical correlation between Stage 0 recovery distances and the Stage 1 instrument.

Stage 2: fixed-effects IV model

The structural equation is:

$$log(H_{ct}) = \alpha + \lambda\widehat{P}_{ct} + X_{ct}\gamma + \mu_c + \tau_t + \varepsilon_{ct} \quad (2)$$

where H_{ct} is the firearm homicide rate per 100,000 residents, $\widehat{P}_{ct}$ is the instrumented drug-price index, and ε_{ct} is clustered by city. The coefficient λ captures the effect of a one-standard-deviation change in instrumented drug prices on the log homicide rate for high-exposure complier cities. OLS fixed-effects specifications using the non-instrumented market index are reported as benchmarks. They are not interpreted causally; they are used to show how IV estimates differ from naive fixed-effects associations. The Wu–Hausman test was also reported, but interpreted cautiously given the limited sample size.

Identification diagnostics and falsification tests

Placebo and falsification tests used the same instrumental-variables structure as the main analysis. Each test replaced firearm homicide with a placebo or falsification outcome and estimated its association with the instrumented integrated drug-price index, using the same controls, city fixed effects, and year fixed effects as the primary specification. This approach tests whether the same instrumented price variation used in the main analysis also predicts outcomes it should not plausibly affect.

The placebo outcomes were selected because they should not be directly caused by annual drug-price variation, but may still reflect the city-year confounding environment that threatens identification. Officers per capita and homicide clearance rate were used as enforcement-placebo outcomes. Police staffing and homicide clearance are not expected to respond directly to annual drug-price fluctuations, but they may capture enforcement intensity, investigative capacity, policing strategy, or municipal public-safety responses. Because both variables are included as controls in the main models, these placebo tests assess whether the instrumented drug-price index also predicts the enforcement environment itself.

Lagged firearm homicide was used as a pre-trend placebo. Current-year drug prices cannot cause prior-year firearm homicide, but lagged homicide captures persistent violence conditions, local firearm availability, gang conflict, and city-specific violence trajectories. Fatal motor vehicle crash rate was used as a broader city-year shock falsification outcome. Drug prices have no clear market-level mechanism linking them to annual fatal crashes, but fatal crashes may reflect broader city-year conditions such as enforcement intensity, risk-taking behavior, economic activity, traffic exposure, or reporting shocks.

Null placebo and falsification results do not prove the exclusion restriction. They reduce concern that the IV estimates are driven by enforcement environment changes, pre-existing violence trajectories, or broad city-year shocks unrelated to drug-price variation.

Spatial robustness

The fixed-effects IV model treats cities as independent conditional on controls and clustering. Three model tiers test that assumption. **Model A** is the PLM 2SLS benchmark. **Model B** adds city and year random intercepts via INLA without a spatial field. **Model C** extends Model B with a continuous-space Matérn spatial field estimated via SPDE with AR(1) temporal dynamics,[31,32] absorbing residual geographic clustering not captured by city fixed effects. The change in WAIC between Models B and C quantifies whether the spatial field improves fit, and Moran's I tests on OLS residuals provide a formal pre-test for spatial dependence. Changes in point estimates across the three tiers — not standard errors — are the primary diagnostic for spatial confounding. The sign of those point estimates is reported without prior expectation.

IV. Results

4.1 Analytic sample and descriptive statistics

Descriptive statistics for the six-city high-exposure sample are reported in Table 3.2. The mean firearm homicide rate was 9.8 per 100,000 residents (SD, 4.2), with values ranging from 2.3 to 20.7. Mean homicide clearance was 0.650, mean officers per capita was 4,186 per 100,000 residents, and mean real per capita personal income was $52,272. Raw observed DEA prices were highly dispersed, particularly for heroin and fentanyl. Figure 3.1 shows substantial within-city and across-city variation in firearm homicide over the study period.

Table 3.2. Summary statistics, six-city high-exposure analytic sample, 2016–2023.

Variable	N	Mean	SD	Median	Min	Max
A. Outcome						
Firearm homicide rate, per 100,000	48	9.8	4.2	9.4	2.3	20.7
B. Raw observed DEA drug prices						
Cocaine price, $/gram	34	102	160	91	42	990
Heroin price, $/gram	25	1,077	1,850	671	275	9,835
Fentanyl price, $/gram	24	9,761	19,500	2,950	842	99,238
Methamphetamine price, $/gram	27	20	42	12	2	225
C. Drug-specific seizure measures (instrument inputs)						
Cocaine seizures, lbs	48	57,700	23,201	58,284	2,226	95,772
Methamphetamine seizures, lbs	48	76,694	58,652	60,897	5,655	177,697
Heroin seizures, lbs	48	63,227	5,186	63,330	50,308	71,998
Fentanyl seizures, lbs	48	5,847	8,169	2,139	5	27,028
D. Covariates						
Homicide clearance rate	48	0.650	0.188	0.670	0.152	1.162
Officers per capita, per 100,000	48	4,186	2,723	2,973	1,731	10,002
Real per capita personal income, $	48	52,272	5,103	52,538	40,654	60,779
Unemployment rate, %	48	5.1	1.7	4.6	3.1	11.4
Poverty rate	48	0.173	0.033	0.171	0.110	0.236
Total population	48	2,004,876	925,344	1,534,629	1,257,676	3,999,742
Percent female	48	0.502	0.005	0.502	0.488	0.509
Percent Black	48	0.127	0.078	0.082	0.055	0.251
Percent Hispanic	48	0.453	0.103	0.438	0.290	0.664

Variable	N	Mean	SD	Median	Min	Max
Percent Asian	48	0.077	0.052	0.054	0.026	0.182
Percent aged 15–24	48	0.142	0.007	0.141	0.128	0.156
Percent aged 25–34	48	0.176	0.012	0.180	0.154	0.198
Percent married	48	0.413	0.018	0.415	0.384	0.448
High school diploma or higher (adults 18+)	48	0.819	0.041	0.811	0.751	0.912
Bachelor's degree or higher (adults 18+)	48	0.312	0.062	0.301	0.217	0.471

Notes: City-year variables are summarized over the six-city high-exposure analytic sample (N = 48 city-year observations; 6 cities × 8 years). Raw DEA drug-price summaries reflect only city-year-drug cells with at least one observed transaction; sample sizes therefore vary by substance. Prices are purity-adjusted dollars per gram of pure substance prior to summarization. Recovered prices and drug-price indices, produced in the Stage 0 spatiotemporal recovery step, are not shown here. Drug-family seizure instruments are constructed from the drug-specific seizure measures shown in Panel C. SD = standard deviation.

Figure 3.1. *City-specific firearm homicide rates in six high-exposure U.S. cities, 2016–2023. Annual firearm homicide rates per 100,000 residents are shown separately for Dallas, Houston, Los Angeles, Phoenix, San Antonio, and San Diego.*

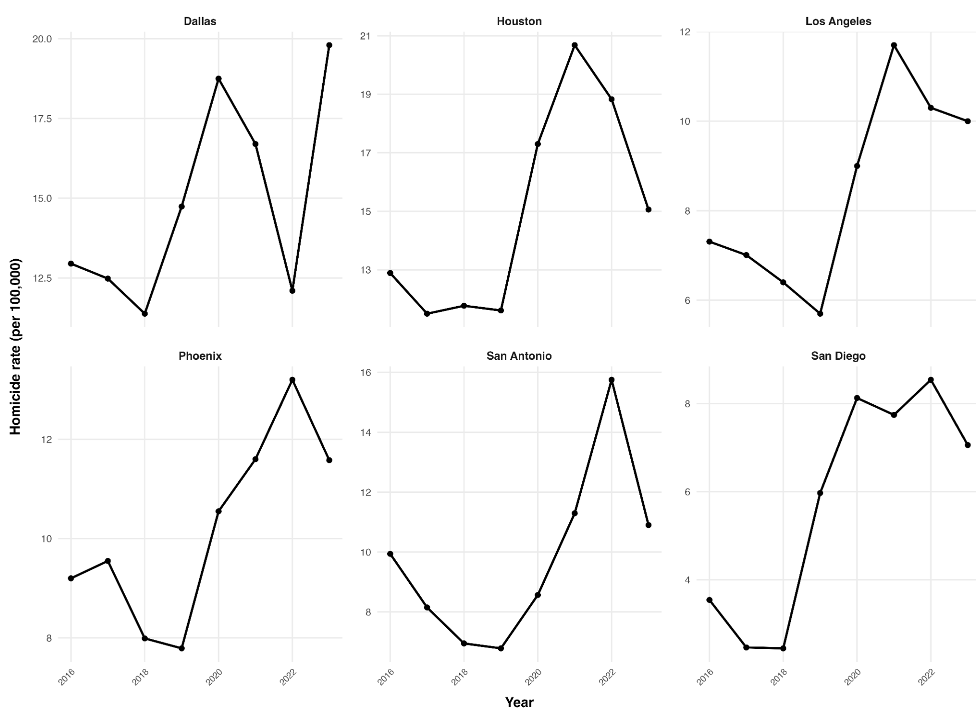

4.2 DEA coverage and Stage 0 recovery

The six-city analytic panel contained 192 possible city-year-drug cells. Of these, 121 (63.0%) included at least one DEA transaction, and 75 (39.1%) met the three-transaction reliability threshold (Table 3.3). The remaining 117 cells (60.9%) required Stage 0 recovery, including 71 unobserved cells and 46 observed but sparse cells.

Table 3.3. DEA transaction coverage in the six-city analytic sample before Stage 0 recovery, 2016–2023.

Category	Count	Percent
Total possible city-year-drug cells	192	100.0
Cells with any DEA transaction	121	63.0
Cells meeting reliability threshold, ≥3 transactions	75	39.1
Cells with no DEA transaction	71	37.0
Observed but sparse cells, <3 transactions	46	24.0
Cells requiring Stage 0 recovery	117	60.9

Notes: The six-city analytic panel contains 192 possible city-year-drug cells, corresponding to six cities observed annually from 2016 to 2023 across four drugs. Percentages are calculated relative to all possible cells. A cell was classified as observed if at least one DEA transaction was available and as reliable if at least three transactions were available. Cells requiring Stage 0 recovery include both completely unobserved cells and observed but sparse cells that did not meet the reliability threshold. DEA = Drug Enforcement Administration.

Stage 0 recovered held-out log prices with high accuracy for cocaine, heroin, and methamphetamine, and with somewhat lower but still strong accuracy for fentanyl (Table 3.4). Pearson correlations between observed and predicted prices were 0.97 for cocaine, 0.96 for heroin, 0.98 for methamphetamine, and 0.89 for fentanyl. Figure 3.2 shows that interpolated prices were less dispersed than raw observed prices, and Figure 3.3 shows the resulting integrated, opioid, and stimulant index trajectories by city.

Table 3.4. Stage 0 spatiotemporal price recovery performance.

Drug	Pearson r	RMSE ($/gram)	MAE ($/gram)
Cocaine	0.97	34	38
Fentanyl	0.89	3,615	3,005
Heroin	0.96	431	216
Methamphetamine	0.98	4	4

Notes: Predictive performance was evaluated using a 20% random holdout sample of observed DEA price cells. Pearson r compares observed and predicted purity-adjusted prices. RMSE = root mean squared error; MAE = mean absolute error.

Figure 3.2. *Observed and interpolated drug-price distributions in the six-city high-exposure sample, 2016–2023.*

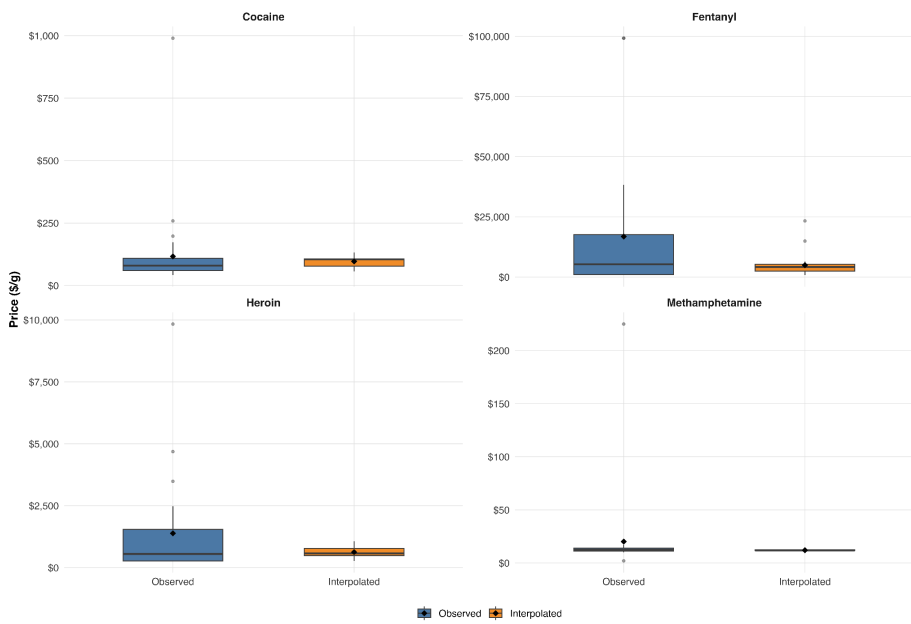

Figure 3.3. *Recovered drug-price indices by city in six high-exposure U.S. cities, 2016–2023.*

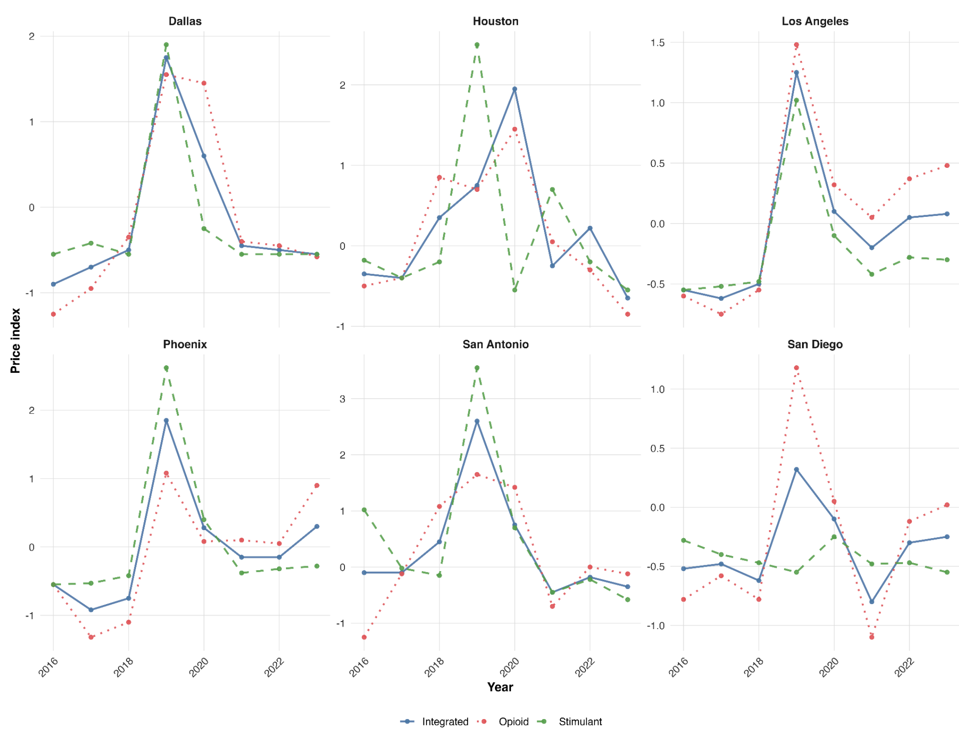

4.3 First-stage relevance and weak-instrument diagnostics

First-stage coefficients on log seizures were positive and statistically distinguishable from zero in all three specifications (Table 3.5). The coefficient was 0.527 (SE, 0.0231) for the integrated index, 0.482 (SE, 0.0772) for the opioid index, and 0.518 (SE, 0.0983) for the stimulant index. The corresponding first-stage F-statistics were 520.3, 39.0, and 27.8. All three exceeded the Stock–Yogo benchmark and the Olea–Pflueger thresholds associated with less than 10% worst-case relative bias; the integrated and opioid models also exceeded the 5% threshold, whereas the stimulant model did not.

The Wu–Hausman test did not reject exogeneity in any specification ($p = 0.104$ for the integrated model, 0.439 for the opioid model, and 0.403 for the stimulant model). Because the main seizure-only specifications were just-identified, Sargan tests were not applicable. Figure 3.4 plots the integrated first-stage relationship, and Figure 3.5 shows the corresponding opioid and stimulant first-stage relationships. Full covariate estimates for first-stage and outcome models are reported in eTable 3.1. Because these coefficients are included for adjustment rather than substantive interpretation, the main text focuses on the drug-price estimates, instrument diagnostics, and spatial model comparisons.

Table 3.5. First-stage results and weak-instrument diagnostics.

	Integrated index	Opioid index	Stimulant index
Log seizures (coefficient)	0.527***	0.482***	0.518***
Standard error	(0.0231)	(0.0772)	(0.0983)
First-stage strength			
First-stage t-statistic	22.81	6.24	5.27
First-stage F-statistic	520.3	39.0	27.8
Weak-instrument test p-value	<0.001	<0.001	<0.001
Relative-bias thresholds (Stock–Yogo)			
Minimum F for bias <30%	8.1	8.1	8.1
Minimum F for bias <20%	11.4	11.4	11.4
Minimum F for bias <10%	18.7	18.7	18.7
Minimum F for bias <5%	29.6	29.6	29.6
Meets 20% bias threshold?	Yes	Yes	Yes
Meets 10% bias threshold?	Yes	Yes	Yes
Meets 5% bias threshold?	Yes	Yes	No
Additional IV diagnostics and model features			
Wu–Hausman p-value	0.104	0.439	0.403
Sargan p-value	N/A	N/A	N/A
R-squared	0.890	0.813	0.841
N	48	48	48
City fixed effects	Yes	Yes	Yes
Year fixed effects	Yes	Yes	Yes
Time-varying controls	Yes	Yes	Yes

Notes: First-stage coefficients on log seizures with standard errors in parentheses. The dependent variable is the relevant city-year drug-price index. The integrated model uses log total drug seizures as the excluded instrument; the opioid and stimulant models use log opioid seizures and log stimulant seizures, respectively. In just-identified specifications, the first-stage F equals the squared first-stage t. Relative-bias thresholds give the minimum F required to bound worst-case IV bias relative to OLS at the listed level. Wu–Hausman tests the null of exogeneity. Sargan tests are not applicable for just-identified models. All models include city and year fixed effects and time-varying controls. * $p < 0.05$, ** $p < 0.01$, *** $p < 0.001$.

Figure 3.4. *First-stage relationship between total drug seizures and the integrated drug-price index in six high-exposure U.S. cities, 2016–2023.*

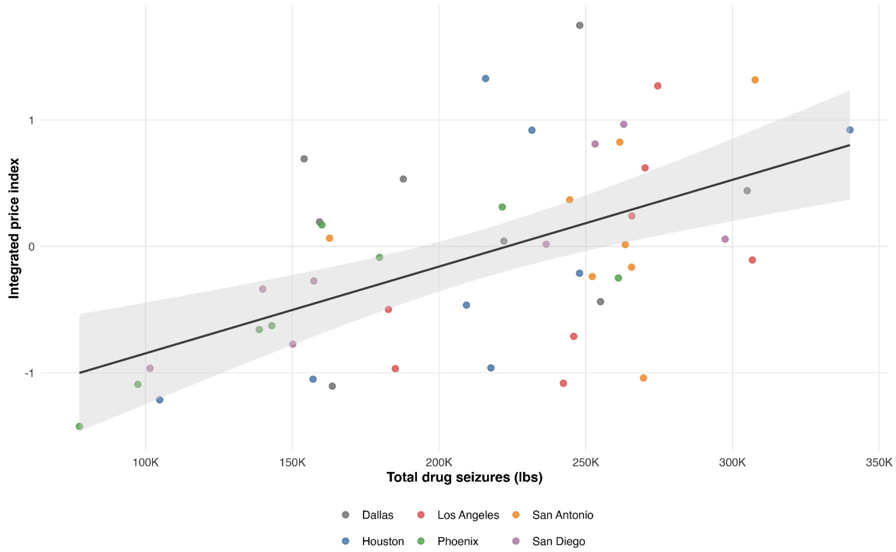

Figure 3.5. *First-stage relationships between family-specific drug seizures and family-specific drug-price indices in six high-exposure U.S. cities, 2016–2023.*

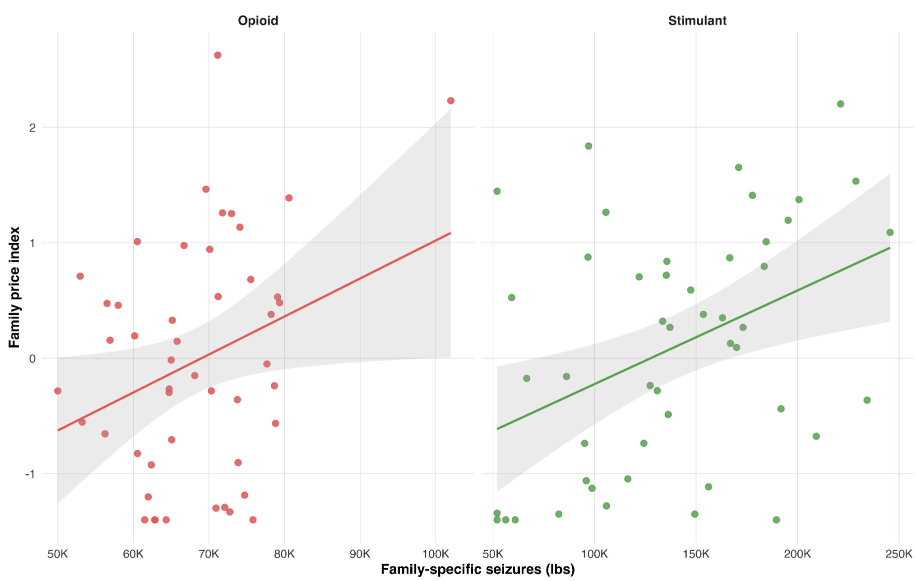

4.4 Placebo and falsification evidence

None of the placebo or falsification outcomes was associated with the seizure instrument (Table 3.6). Log seizures did not predict officers per capita (β = 0.011, p = 0.391), homicide clearance (β = 0.022, p = 0.762), the lagged firearm homicide rate (β = 0.011, p = 0.707), or the city-year fatal motor vehicle crash rate (β = 0.022, p = 0.707).

Table 3.6. Placebo and falsification tests.

Test outcome	Predictor	Estimate	SE	p-value
Enforcement placebo: officers per capita	Instrumented drug-price index	0.0291	0.0598	0.627
Enforcement placebo: homicide clearance rate	Instrumented drug-price index	0.0252	0.0515	0.625
Pre-trend placebo: lagged firearm homicide rate	Instrumented drug-price index	0.0166	0.0267	0.534
Falsification outcome: fatal crash rate	Instrumented drug-price index	0.0127	0.0491	0.796

Notes: Entries are coefficients, standard errors, and p-values from placebo and falsification models that use the same IV structure as the main analysis, replacing firearm homicide with the listed outcome. The predictor is the instrumented integrated drug-price index; log total drug seizures is the excluded instrument. All models include city and year fixed effects and the full set of time-varying controls. Officers per capita and homicide clearance rate are also controls in the main models and are examined here as enforcement-placebo outcomes. Null associations do not prove the exclusion restriction, but they reduce concern that the IV estimates are driven by enforcement intensity, pre-existing violence trends, or broad city-year shocks. SE = standard error.

4.5 Estimated effects of instrumented drug prices on firearm homicide

Estimated effects of instrumented drug prices on firearm homicide are reported in Table 3.7 and summarized visually in Figure 3.6. In the OLS fixed-effects benchmark, the coefficient on the integrated index was small and not distinguishable from zero ($\beta = -0.018$; 95% CI, −0.042 to 0.006).

Table 3.7. Estimated effects of instrumented drug prices on firearm homicide across model specifications

Model	Estimate	SE / SD	95% interval	WAIC
A. Linear and panel IV models				
OLS fixed effects	−0.018	0.012	[−0.042, 0.006]	—
PLM-2SLS, integrated index	−1.676	0.714	[−3.075, −0.277]	—
PLM-2SLS, opioid index	−0.676	0.591	[−1.834, 0.482]	—
PLM-2SLS, stimulant index	−2.848	0.624	[−4.071, −1.625]	—
B. INLA models with temporal random effects				
INLA time-only, integrated index	−1.671	0.796	[−3.872, 0.608]	1232.1
INLA time-only, opioid index	−0.676	0.524	[−2.998, 0.311]	1247.3
INLA time-only, stimulant index	−2.849	0.688	[−4.720, −2.018]	1210.8
C. INLA models with spatiotemporal random effects				
INLA spatiotemporal, integrated index	−1.804	0.916	[−4.463, 0.252]	1007.6
INLA spatiotemporal, opioid index	−0.792	0.604	[−3.030, 0.232]	1099.6
INLA spatiotemporal, stimulant index	−2.947	0.755	[−4.763, −2.158]	979.5

Notes: OLS and PLM-2SLS entries report coefficient estimates with standard errors and 95% confidence intervals. INLA entries report posterior means, posterior standard deviations, 95% credible intervals, and WAIC. Lower WAIC indicates better model fit among Bayesian models only.

Figure 3.6. *Estimated effects of instrumented drug prices on firearm homicide across model specifications in six high-exposure U.S. cities, 2016–2023.*

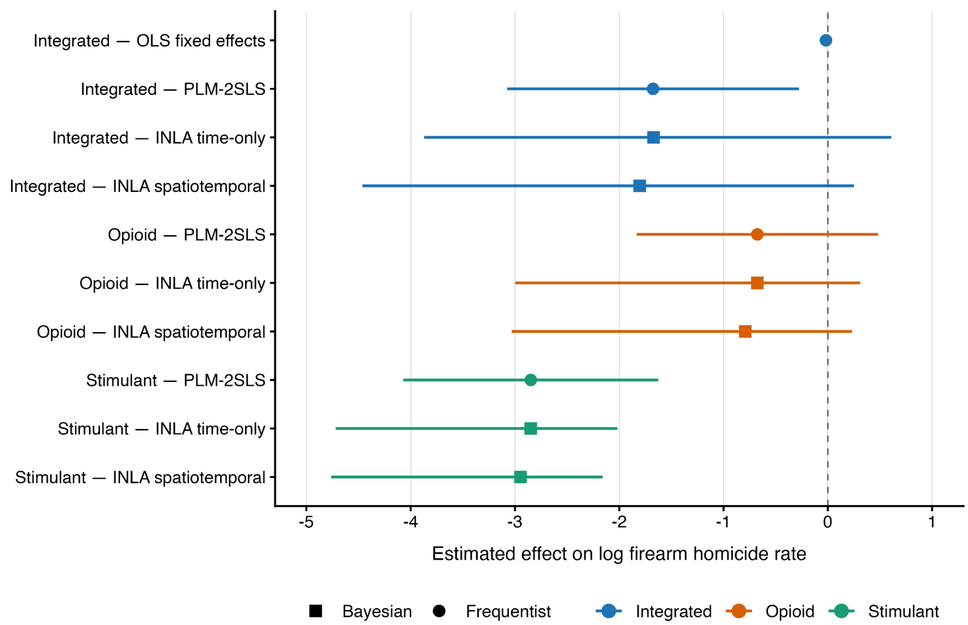

Panel IV estimates were larger in magnitude and negative across all three indices: −1.676 (95% CI, −3.075 to −0.277) for the integrated index, −0.676 (95% CI, −1.834 to 0.482) for the opioid index, and −2.848 (95% CI, −4.071 to −1.625) for the stimulant index.

The INLA time-only models produced posterior means similar to the panel IV estimates: −1.671 for the integrated index, −0.676 for the opioid index, and −2.849 for the stimulant index. The corresponding 95% credible intervals were [−3.872, 0.608], [−2.998, 0.311], and [−4.720, −2.018].

In the spatiotemporal INLA models, posterior means remained negative across all three indices: −1.804 for the integrated index, −0.792 for the opioid index, and −2.947 for the stimulant index. The corresponding 95% credible intervals were [−4.463, 0.252], [−3.030, 0.232], and [−4.763, −2.158].

4.6 Spatial robustness

The spatiotemporal models fit the data substantially better than the time-only Bayesian benchmarks (Table 10). WAIC declined by 224.5 points for the integrated model, 147.7 points for the opioid model, and 231.3 points for the stimulant model. Estimated practical spatial ranges were 233 miles (95% CrI, 115 to 428) for the integrated model, 226 miles (95% CrI, 112 to 411) for the opioid model, and 223 miles (95% CrI, 112 to 407) for the stimulant model. Marginal spatial standard deviations were similar across specifications, ranging from 2.63 to 2.68. Temporal AR(1) coefficients were approximately 0.36 to 0.37 in all three models. These hyperparameter estimates are reported for completeness; given the small number of cities in the analytic sample, they should be interpreted as model diagnostics rather than reliable estimates of the spatial correlation structure. Residual spatial autocorrelation was evident in the non-spatial benchmark models but was largely eliminated after inclusion of the spatiotemporal random effect (Table 3.8). Moran's I values in the non-spatial benchmarks were 0.369, 0.266, and 0.421 for the integrated, opioid, and stimulant models, respectively, all with $p < 0.001$. After fitting the spatiotemporal models, the corresponding Moran's I values were 0.021, 0.018, and 0.011, all statistically nonsignificant.

Table 3.8. Spatial-model hyperparameters and residual spatial dependence diagnostics.

Measure	Integrated index	Opioid index	Stimulant index
A. Spatial-field hyperparameters			
Practical range, ρ (miles)	233.1 [114.7, 427.8]	225.5 [112.2, 411.1]	223.4 [112.0, 406.8]
Marginal spatial SD, σ	2.63 [2.09, 3.29]	2.68 [2.11, 3.35]	2.68 [2.12, 3.36]
Temporal AR(1) correlation, ϕ	0.36 [0.09, 0.59]	0.37 [0.09, 0.60]	0.37 [0.09, 0.60]
Residual SD, σ_ε	0.01 [0.00, 0.02]	0.01 [0.00, 0.03]	0.01 [0.00, 0.02]
B. Residual spatial autocorrelation (Moran's I)			
Non-spatial benchmark	0.369 ($p < 0.001$)	0.266 ($p < 0.001$)	0.421 ($p < 0.001$)
Spatiotemporal model	0.021 ($p = 0.412$)	0.018 ($p = 0.337$)	0.011 ($p = 0.529$)
C. Model fit improvement			
WAIC, time-only model	1232.1	1247.3	1210.8
WAIC, spatiotemporal model	1007.6	1099.6	979.5
ΔWAIC, time-only to spatiotemporal	−224.5	−147.7	−231.3

Notes: Hyperparameters are reported as posterior means with 95% credible intervals. Practical range is the distance at which spatial correlation falls to approximately 0.139. Moran's I was calculated on model residuals using the prespecified spatial weights matrix; positive values indicate residual clustering. Lower and statistically nonsignificant Moran's I after fitting the spatiotemporal model indicates that the spatial random effect absorbed residual spatial dependence. ΔWAIC is the spatiotemporal WAIC minus the time-only WAIC; negative values indicate improved fit after adding the spatial field. WAIC = Watanabe–Akaike information criterion; SD = standard deviation.

V. Discussion

This study examined whether exogenous changes in illicit drug prices influenced firearm homicide in six high-exposure U.S. cities during the 2016–2023 fentanyl restructuring era. Because market-conflict and market-contraction mechanisms imply opposing predictions, the sign of the effect was left open ex ante. The estimates were negative across the integrated, opioid, and stimulant drug-price indices, providing no support for the hypothesis that higher instrumented drug prices increase firearm homicide in this setting. DEA transaction coverage was incomplete even in this restricted sample, and most city-year-drug cells required recovery before index construction. Seizure-based first stages were strong across all three drug-price definitions, and placebo and falsification tests did not indicate that the instrument was proxying enforcement intensity, pre-existing violence trends, or broad city-year shocks.

The negative direction of the estimates is closer to DeSimone's U.S. evidence on cocaine prices and murder than to the positive homicide response to supply contraction reported by Castillo and colleagues in Mexico.[10,12] The contrast likely reflects differences in setting, time scale, and market organization. Castillo's setting involved an active drug war and contested control over trafficking rents, whereas the present sample consists of established U.S. urban markets in the synthetic-opioid era, where supply-side disruption may operate through different channels and annual data may average over shorter-run conflict responses.

Substantively, the negative estimates are more consistent with a market-contraction interpretation than with a dominant market-conflict mechanism. Under this interpretation, higher instrumented drug prices may reflect supply-side pressure that reduces consumption among price-responsive users, contracts illicit transaction volume, and reduces the number of disputed exchanges — including debt enforcement, territorial conflict, and contested transactions — that can generate systemic firearm violence. This logic requires demand to be at least partially price-elastic, a condition that prior evidence on cocaine and stimulant markets suggests is plausible. The stimulant estimates were the most precise and stable across model tiers, which may reflect greater demand responsiveness or more contestable territorial structure in stimulant markets relative to opioid markets in this period. The opioid estimates were consistently negative but less precise, leaving the opioid mechanism unresolved. These interpretations remain suggestive: the design identifies the effect of instrumented drug prices, not whether the pathway operates through lower transaction volume, reduced dispute intensity, displacement, selective enforcement, or other market responses.

The spatiotemporal models improved fit substantially relative to the time-only benchmarks across all three indices, and residual Moran's I values — large and significant in the non-spatial models — fell to near zero after the spatial field was added. These results indicate that residual spatial dependence was present and that the spatiotemporal specification absorbed it. Point estimates remained negative and of comparable magnitude across all three model tiers, supporting the stability of the primary PLM-2SLS estimates. Given the small number of cities in the analytic sample, the practical-range hyperparameter estimates are reported in Table 3.8 as model diagnostics rather than substantive findings.

These findings carry both substantive and methodological implications. Substantively, the results do not support the view that higher instrumented drug prices uniformly increase firearm homicide in high-exposure U.S. cities during the fentanyl era. Methodologically, they show that city-panel studies of drug prices and violence may mischaracterize fit and uncertainty when residual spatial dependence is ignored. The large WAIC improvements and near-disappearance of residual Moran's I after spatial adjustment indicate that residual geographic clustering was present and meaningfully absorbed by the spatiotemporal specification.

The study has several strengths. It combines a sparse-data recovery step, explicit instrument separation, a high-exposure subsample chosen to strengthen the first stage, and a tiered spatial robustness framework. The seizure instrument performed well under conventional and clustered-robust weak-instrument diagnostics. The placebo and falsification tests were uniformly null. Full model results, including covariate significance patterns, are provided in eTable 3.1, allowing the main text to focus on the primary estimands rather than secondary coefficients.

Several limitations qualify interpretation. The analytic panel was small, with 48 city-year observations, which limits precision, especially for the opioid models. DEA STRIDE data are not random samples of retail market prices, and although the recovery step performed well in holdout validation, the resulting price indices remain modeled quantities. Annual data may also be too coarse to detect short-run organizational shocks, retaliation cycles, or abrupt supply disruptions. The stimulant first stage did not meet the most stringent weak-instrument relative-bias threshold, although it comfortably exceeded the conventional and 10% benchmarks. Finally, the design identifies the effect of instrumented drug prices, not the specific pathway through which price changes affect homicide. The estimates cannot distinguish among reduced transaction volume, reduced dispute intensity, displacement, selective survival, selective enforcement, or other within-market mechanisms.

The policy implication is not that enforcement should be intensified or that higher drug prices are inherently violence-reducing. Rather, the violence effects of supply disruption should be treated as empirical and setting-specific rather than assumed. In this high-exposure sample, the estimates do not support the hypothesis that higher instrumented drug prices increase firearm homicide. The consistently negative estimates suggest a possible market-contraction channel, but the study cannot determine whether that channel reflects reduced transaction volume, fewer disputes, displacement, or another mechanism. This distinction matters for synthetic-era policy debates that ask whether supply suppression produces collateral violence harms, collateral violence benefits, or neither.[23,24]

In summary, exogenous increases in illicit drug prices were not associated with increases in firearm homicide in six high-exposure U.S. cities during 2016–2023. Point estimates were negative across all three drug-price indices, with the strongest and most stable evidence in the stimulant specification. These findings do not support a dominant market-conflict mechanism in this setting and are more consistent with, but do not prove, a market-contraction interpretation. Future work should test these mechanisms at finer temporal scales and in larger city panels where short-run retaliation, displacement, and organizational responses can be observed more directly.

References

1. Garnett MF, Miniño AM. Drug overdose deaths in the United States, 2003–2023. NCHS Data Brief No. 522. Hyattsville, MD: National Center for Health Statistics; 2024. DOI: 10.15620/cdc/170565.
2. Centers for Disease Control and Prevention. WISQARS Fatal Injury Data. Accessed 2024.
3. Peterson C, Luo F, Florence C. State-level economic costs of fatal injuries — United States, 2019. *MMWR Morb Mortal Wkly Rep*. 2021;70:1660–1663.
4. Martínez R, Rosenfeld R, Mares D. Social disorganization, drug market activity, and neighborhood violent crime. *Urban Aff Rev*. 2008;43(6):846–874.
5. Goldstein PJ. The drugs/violence nexus: a tripartite conceptual framework. *J Drug Issues*. 1985;15(4):493–506.
6. Friedman J, Ciccarone D. The public health risks of counterfeit pills. *Lancet Public Health*. 2025;10(1):e58–e62.
7. Harris E. US deaths from overdoses involving fake pills have increased. *JAMA*. 2023;330(13):1217.
8. Cumming C, Kinner SA, McKetin R, Li I, Preen D. Methamphetamine use, health and criminal justice system outcomes: a systematic review. *Drug Alcohol Rev*. 2020;39(5):505–518.
9. United States Attorney's Office, SDNY. U.S. Attorney announces charges against 18 defendants in scheme to manufacture and distribute millions of deadly counterfeit pharmaceuticals through fake online pharmacies. Press release; September 30, 2024.
10. Castillo JC, Mejía D, Restrepo P. Scarcity without Leviathan: the violent effects of cocaine supply shortages in the Mexican drug war. SSRN Working Paper; 2018. DOI: 10.2139/ssrn.2409268.
11. Payne J, Manning M, Fleming C, Pham H. The price elasticity of demand for illicit drugs: a systematic review. *Trends Issues Crime Crim Just*. No. 606. Canberra: Australian Institute of Criminology; 2020.
12. DeSimone J. The effect of cocaine prices on crime. *Econ Inq*. 2001;39(4):627–643.
13. Felson RB, Staff J. Committing economic crime for drug money. *Crime Delinq*. 2017;63(4):375–390.
14. Sarrica F. Drug prices and systemic violence: an empirical study. *Eur J Crim Pol Res*. 2008;14:391–415.
15. Martínez R, Rosenfeld R, Mares D, 2008. [See reference 4.]
16. Park S. The growth of illicit drug use and its effects on murder rates. *Health Econ*. 2025;34(3):456–471.
17. Friedman J, Ciccarone D, 2025. [See reference 6.]
18. White CM. Counterfeit drugs: a major issue for vulnerable citizens throughout the world and in the United States. *J Am Pharm Assoc*. 2021;61(1):e93–e98.
19. Friedman J, Ciccarone D, 2025. [See reference 6.]
20. Caulkins JP, Reuter P. What price data tell us about drug markets. *J Drug Issues*. 1998;28(3):593–612.
21. Fries A, Anthony RW, Cseko A, Gaither CC, Schulman E. *The Price and Purity of Illicit Drugs: 1981–2007*. Alexandria, VA: Institute for Defense Analyses; 2008.

22. Arkes J, Pacula RL, Paddock SM, Caulkins JP, Reuter P. Why the DEA STRIDE data are still useful for understanding drug markets. NBER Working Paper 14224; 2008.
23. Moeller K, Sandberg S. Putting a price on drugs: an economic sociological study of price formation in illegal drug markets. *Criminology*. 2019;57(2):289–313.
24. Osorio J. The contagion of drug violence: spatiotemporal dynamics of the Mexican War on Drugs. *J Conflict Resolut*. 2015;59(8):1403–1432.
25. Conley TG. GMM estimation with cross sectional dependence. *J Econometrics*. 1999;92(1):1–45.
26. Cameron AC, Miller DL. A practitioner's guide to cluster-robust inference. *J Hum Resour*. 2015;50(2):317–372.
27. Caulkins JP. How should drug policy respond to surging supplies of dangerous drugs? Brookings Institution; December 2024.
28. Robles G, Calderón G, Magaloni B. *Economic Consequences of Drug-Trafficking Violence in Mexico*. IDB Working Paper IDB-WP-426. Washington, DC: Inter-American Development Bank; 2013.
29. Clarke RV, Cornish DB. Analyzing organized crimes. In: Piquero AR, Tibbets SG, eds. *Rational Choice and Criminal Behavior*. New York: Routledge; 2001:69–90.
30. Dalal AJ, Raju S. Decision-making under risk in the market for illegal drugs: a supply-side analysis. *Bull Econ Res*. 2024.
31. Lindgren F, Rue H, Lindström J. An explicit link between Gaussian fields and Gaussian Markov random fields: the SPDE approach. *J R Stat Soc B*. 2011;73(4):423–498.
32. Lindgren F, Rue H. Bayesian spatial modelling with R-INLA. *J Stat Softw*. 2015;63(19):1–25.
33. Stock JH, Yogo M. Testing for weak instruments in linear IV regression. In: Andrews DWK, Stock JH, eds. *Identification and Inference for Econometric Models: Essays in Honor of Thomas Rothenberg*. Cambridge University Press; 2005:80–108.
34. Agreement between the United States of America and the United Mexican States on Cooperation for the Protection and Improvement of the Environment in the Border Area (La Paz Agreement), signed at La Paz, Baja California Sur, August 14, 1983. T.I.A.S. 10827.
35. Olea JLM, Pflueger C. A robust test for weak instruments. *J Bus Econ Stat*. 2013;31(3):358–369. DOI: 10.1080/00401706.2013.806694.

Chapter 3 Appendix

eTable 3.1 reports full covariate estimates for the first-stage models (Panel A) and the second-stage outcome models (Panel B). Panel A includes the four frequentist first-stage specifications. Panel B is presented in landscape orientation to accommodate all seven main-text outcome specifications (OLS fixed effects, three PLM-2SLS models, one INLA time-only model, and two INLA spatiotemporal models) in a single table.

eTable 3.1.A. Full first-stage model results.

Variable	Integrated index	Opioid index	Stimulant index
Log seizures	0.527*** (0.023)	0.482*** (0.077)	0.518*** (0.098)
log(Population)	0.0162 (0.0139)	0.0291** (0.0098)	0.0262* (0.0109)
Unemployment rate	0.024 (0.022)	0.024 (0.012)	0.021 (0.019)
log(PCPI)	1.192*** (0.091)	1.031*** (0.095)	1.353*** (0.087)
log(Clearances)	−0.0069 (0.0167)	−0.0067 (0.0106)	−0.0031 (0.0124)
Poverty rate	0.1194 (0.2008)	0.1456 (0.2021)	0.1158 (0.1925)
Percent female	−0.3235 (0.2132)	−0.3068 (0.3495)	−0.2885 (0.3003)
Percent Black	−0.1317 (0.2404)	−0.1713 (0.2403)	−0.1539 (0.2649)
Percent Hispanic	0.1396 (0.2404)	0.1443 (0.2403)	0.0836 (0.2649)
Percent married	0.3611 (0.3041)	0.4163 (0.3555)	0.3549 (0.3446)
Percent aged 15–24	0.0862 (0.6145)	0.1536 (0.5412)	0.0493 (0.6022)
Percent aged 25–34	0.1355 (0.5509)	0.0968 (0.5689)	0.1661 (0.6026)
High school completion rate	−0.0322 (0.3223)	−0.0046 (0.2831)	−0.0505 (0.3412)
Bachelor's degree rate	−0.0250 (0.2062)	−0.0700 (0.1878)	−0.0380 (0.1880)
log(Officers)	−0.0253 (0.0555)	−0.0258 (0.0462)	−0.0160 (0.0480)
City fixed effects	Yes	Yes	Yes
Year fixed effects	Yes	Yes	Yes
N	48	48	48

Notes: The dependent variable is the relevant city-year drug-price index. The integrated model uses log total drug seizures as the excluded instrument; the opioid model uses log heroin and fentanyl seizures; and the stimulant model uses log cocaine and methamphetamine seizures. All models include city fixed effects, year fixed effects, and the full set of time-varying controls. * $p < 0.05$, ** $p < 0.01$, *** $p < 0.001$.

eTable 3.1.B Full second-stage model results.

Variable	OLS-FE	2SLS Int.	2SLS Op.	2SLS Stm.	INLA Time Int.	INLA ST Int.	INLA ST Stm.
Drug-price index	−0.018 (0.012)	−1.676* (0.714)	−0.676 (0.591)	−2.848*** (0.624)	−1.671 [−3.872, 0.608]	−1.804 [−4.463, 0.252]	−2.947 [−4.763, −2.158]
log(Population)	0.0693*** (0.0135)	0.0398*** (0.0104)	0.0870*** (0.0115)	0.0535*** (0.0126)	0.052 [0.018, 0.086]	0.044 [0.006, 0.082]	0.041 [0.001, 0.081]
Unemployment rate	0.1200 (0.1070)	0.0910 (0.0816)	0.0730* (0.0290)	0.1000 (0.0850)	0.043 [−0.118, 0.204]	0.031 [−0.149, 0.211]	0.022 [−0.139, 0.183]
log(PCPI)	0.1920 (0.1290)	0.2954* (0.1490)	0.1381 (0.0825)	0.0989 (0.0982)	0.156 [−0.083, 0.395]	0.132 [−0.141, 0.405]	0.109 [−0.130, 0.348]
log(Clearances)	−0.0023 (0.0015)	−0.0069*** (0.0017)	−0.0067*** (0.0011)	−0.0031* (0.0012)	−0.0048 [−0.0119, 0.0023]	−0.0039 [−0.0121, 0.0043]	−0.0023 [−0.0094, 0.0048]
Poverty rate	0.1453 (0.1036)	0.2194* (0.1020)	0.1560 (0.1020)	0.3580 (0.2019)	0.176 [−0.030, 0.382]	0.143 [−0.097, 0.383]	0.132 [−0.099, 0.363]
Percent female	−0.4825 (0.4481)	−0.3235 (0.2132)	−0.3068 (0.3495)	−0.2885 (0.3003)	−0.386 [−1.135, 0.363]	−0.318 [−1.190, 0.554]	−0.274 [−1.096, 0.548]
Percent Black	−0.1842 (0.2410)	−0.1317 (0.2404)	−0.1713 (0.2403)	−0.1539 (0.2649)	−0.166 [−0.622, 0.290]	−0.122 [−0.672, 0.428]	−0.147 [−0.734, 0.440]
Percent Hispanic	0.2310* (0.1104)	0.1396 (0.1120)	0.1443 (0.1350)	0.0836 (0.0829)	0.167 [−0.046, 0.380]	0.128 [−0.121, 0.377]	0.082 [−0.109, 0.273]
Percent married	0.3196 (0.5170)	0.3611 (0.2041)	0.4163 (0.2555)	0.3549 (0.2446)	0.287 [−0.498, 1.072]	0.244 [−0.642, 1.130]	0.268 [−0.566, 1.102]
Percent aged 15–24	0.1889 (0.5145)	0.0862 (0.6145)	0.1536 (0.5412)	0.0493 (0.6022)	0.211 [−1.010, 1.432]	0.164 [−1.231, 1.559]	0.084 [−1.376, 1.544]
Percent aged 25–34	0.0872*** (0.0222)	0.1355* (0.0551)	0.0968 (0.0569)	0.1661** (0.0603)	0.109 [−0.014, 0.232]	0.087 [−0.060, 0.234]	0.121 [−0.033, 0.275]
High school completion rate	−0.0982 (0.2939)	−0.0322 (0.3223)	−0.0046 (0.2831)	−0.0505 (0.3412)	−0.071 [−0.654, 0.512]	−0.052 [−0.738, 0.634]	−0.041 [−0.728, 0.646]
Bachelor's degree rate	−0.0828 (0.0553)	−0.1250 (0.1226)	−0.0700 (0.0691)	−0.0380 (0.0201)	−0.058 [−0.166, 0.050]	−0.046 [−0.179, 0.087]	−0.036 [−0.138, 0.066]
log(Officers)	−0.0659*** (0.0197)	−0.0253 (0.0155)	−0.0580 (0.0362)	−0.1190 (0.1080)	−0.043 [−0.091, 0.005]	−0.035 [−0.094, 0.024]	−0.031 [−0.104, 0.042]
City fixed effects	Yes	Yes	Yes	Yes	—	—	—
Year fixed effects	Yes	Yes	Yes	Yes	—	—	—
N	48	48	48	48	48	48	48
WAIC	—	—	—	—	1232.1	1007.6	979.5
Practical range, miles	—	—	—	—	—	233.1 [114.7, 427.8]	223.4 [112.0, 406.8]
Marginal spatial SD	—	—	—	—	—	2.63 [2.09, 3.29]	2.68 [2.12, 3.36]
AR(1) correlation	—	—	—	—	0.36 [0.09, 0.59]	0.36 [0.09, 0.59]	0.37 [0.09, 0.60]

Notes: Linear model entries are coefficients with standard errors in parentheses; stars indicate frequentist significance: * $p < 0.05$, ** $p < 0.01$, *** $p < 0.001$. INLA entries are posterior means with 95% credible intervals in brackets and are not assigned significance stars. OLS-FE and 2SLS models include city fixed effects, year fixed effects, and the full set of time-varying controls. INLA time-only models include temporal random effects; INLA spatiotemporal models include a continuous-space Matérn spatial field with AR(1) temporal dynamics. Int. = integrated; Op. = opioid; Stm. = stimulant; ST = spatiotemporal; WAIC = Watanabe–Akaike information criterion.

Chapter 4

General Discussion and Conclusion

Joint Implications of Aims 1 and 2 for Health Economics, Policy, and Spatial Methods

This dissertation examined firearm-related harm in the United States from two complementary vantage points. Chapter 2 estimated mean 30-day treatment costs per treated firearm-injury patient at the county level and assessed how much of the observed geographic inequality was associated with local Medicare reimbursement geography and measured payer-market, demographic, contextual, and health care system factors. Chapter 3 examined whether exogenous changes in illicit drug prices affected firearm homicide in six high-exposure U.S. cities, using seizure-based instruments and spatial robustness checks to assess the stability of inference. The chapters do not estimate a single causal pathway linking drug-price shocks, firearm homicide, and treatment costs. Instead, they provide two related but distinct analyses of firearm-related harm: one downstream analysis of treatment costs and one upstream analysis of drug prices as a market-level condition associated with lethal violence. Their joint contribution is methodological and spatial: both show that policy-relevant firearm outcomes can be recovered from imperfect data, and that both outcomes exhibit geographic structure that exceeds conventional administrative boundaries.

What the Two Aims Jointly Show

First, both aims show that firearm-related harm is geographically structured, but they do so for different outcomes and through different mechanisms. In Aim 1, treatment costs were spatially correlated across an estimated 222 km — a scale more consistent with hospital referral regions, trauma systems, and regional payment environments than with isolated county-level processes. In Aim 2, firearm homicide showed evidence of residual spatial dependence in non-spatial benchmark models, motivating spatial robustness checks rather than a purely independent city-panel interpretation. These findings should not be read as evidence that the same mechanism produces both patterns, that high-homicide regions necessarily have high treatment costs, or that drug-price shocks affect treatment costs. The interpretation is narrower: both outcomes are geographically structured, and county lines and city limits are incomplete units for studying firearm-related harm.

Second, residual spatial dependence is a substantive concern, not merely a modeling detail. In Aim 1, the raw county cost surface was strongly spatially clustered, and the estimated spatial range remained stable across sensitivity analyses. In Aim 2, residual spatial autocorrelation was evident in non-spatial benchmark models, and spatial robustness checks assessed whether the main IV estimates were sensitive to that structure. For firearm-injury costs, ignoring spatial dependence risks overstating the precision of sparse local estimates. For firearm homicide, ignoring spatial dependence risks treating linked cities as independent observations when they may share regional shocks. The broader methodological implication is that fixed effects do not automatically resolve spatial confounding when outcomes are linked through regional systems; city or county fixed effects should be paired with explicit spatial diagnostics and robustness checks.

Third, both aims demonstrate that policy-relevant local quantities can be recovered from imperfect data, but only with explicit assumptions and uncertainty. Aim 1 used claims data with detailed cost information but uneven payer and geographic coverage; it therefore required population calibration, censoring adjustment, geographic harmonization, and Bayesian smoothing. Aim 2 used DEA STRIDE transaction records with informative but sparse price observations; it therefore required Stage 0 spatiotemporal price recovery, explicit separation between price recovery and the seizure-based instrument, and placebo and falsification tests. In both cases, the estimated quantities — county-level mean treatment costs in Aim 1 and city-year drug-price indices in Aim 2 — are modeled quantities. Their value lies not in pretending that the data are complete, but in making the recovery process transparent, testable, and accompanied by uncertainty.

Implications for Health Economics and Policy

Local Cost Measurement and Interpretation

This dissertation contributes a framework for estimating local economic quantities for rare, high-acuity health events. Direct local estimation is often unstable when events are concentrated and sample sizes are small; aggregate estimation is more stable but hides the variation that matters for planning and financing. The same modeled-recovery logic developed for Aim 1 applies to other high-acuity outcomes for which costs are geographically concentrated and unevenly observed in claims data, including severe burns, traumatic brain injury, penetrating trauma, and complex emergency surgical care.

The dissertation also reinforces a basic health economics point: paid treatment costs are not the same as clinical need, treatment intensity, or social burden. In Aim 1, geographic variation in paid costs may reflect reimbursement rules, payer mix, local wage and practice-cost adjustments, trauma-system organization, transfer patterns, injury severity, or coding differences. The analysis therefore does not support a simple ranking of counties as efficient or inefficient. Instead, it provides a geographically explicit cost surface that can be used to ask better questions about where spending is concentrated, where uncertainty is high, and where additional clinical data are needed.

Trauma-System Planning, Payment, and Public Financing

For trauma-system planning, Aim 1 suggests that county-level cost estimates should be interpreted within regional systems of care. A county with high predicted treatment costs may be part of a broader referral network, may receive more severe transferred cases, may face higher local reimbursement rates, or may have a different mix of inpatient and post-acute care. Conversely, a county with lower predicted costs does not necessarily have a lower clinical burden; lower costs may reflect fewer patients surviving to costly treatment, limited access, different coding patterns, or less intensive observed care. The cost surface is therefore best used as a planning baseline, not a performance scorecard.

For payment and financing policy, Aim 1's decomposition is directly relevant. Local Medicare reimbursement geography produced the largest single-step reduction in geographic inequality, and payer mix and insurance-market structure were associated with additional attenuation. However, substantial variation remained after full adjustment: the mean annual P90/P10 ratio declined from 1.86 at baseline to 1.51 in the fully adjusted model, leaving counties near the top of the predicted cost distribution with costs approximately 51% higher than counties near the bottom. Payment geography and payer-market structure therefore capture meaningful but incomplete portions of the observed cost pattern. Because public payers finance a large share of firearm-injury hospital care, these regional cost patterns may matter for Medicaid, Medicare, uncompensated-care financing, trauma-system planning, and safety-net hospitals. However, this dissertation did not estimate payer-specific expenditures or public budget impacts directly. The findings should therefore be read as evidence of geographically structured treatment costs rather than as a payer-specific financing analysis.

Drug Policy and Spatially Connected Violence

For drug policy, Aim 2 supports a narrower and more cautious implication. In the six high-exposure cities studied, higher instrumented drug prices were not associated with higher firearm homicide during 2016 through 2023. Point estimates were negative across the integrated, opioid, and stimulant drug-price indices, with the strongest and most stable evidence in stimulant markets. However, the design cannot identify the precise mechanism behind the negative association, and annual city-level data may average over shorter-run conflict responses. The most defensible policy takeaway is that the violence consequences of supply disruption should be measured rather than assumed. The evidence in this setting does not support a dominant market-conflict mechanism, but it also does not imply that supply-side enforcement is uniformly violence-reducing or welfare-improving.

Limitations Across Both Aims

Several cross-cutting limitations qualify interpretation. The estimated quantities in both aims are modeled rather than directly observed everywhere; validation and sensitivity analyses support these recoveries, but they do not remove all dependence on modeling assumptions.

Aim 1 cannot directly observe injury severity, physiologic status, baseline frailty, or complete trauma registry detail. Residual geographic variation after adjustment therefore cannot be cleanly attributed to delivery-system organization, clinical need, coding intensity, payer contracts, or payment differences. The analysis is descriptive and should not be interpreted as evidence that high-cost counties are inefficient or that low-cost counties provide better care.

Aim 2 is limited by its six-city analytic sample, annual time scale, and focus on high-exposure cities. These features strengthen the relevance of the seizure instrument but limit precision and generalizability. Annual data may miss short-run retaliatory cycles, abrupt supply disruptions, or organizational shocks that unfold over weeks or months. The design estimates the effect of instrumented drug prices, not the specific pathway through which price changes affect homicide.

The two aims also differ in geography, outcome definition, and time period. Aim 1 is a national county-level analysis of treated firearm-injury costs from 2016 through 2024; Aim 2 is a city-level analysis of firearm homicide in six high-exposure cities from 2016 through 2023. Their spatial findings are therefore not directly comparable in a strict numerical sense. Their common implication is qualitative: both outcomes show geographic structure that exceeds the administrative units used in conventional analysis.

Future Research

Several extensions follow from these findings. For Aim 1, the most important next step is linkage between claims and trauma registry data. Such linkage would allow future studies to incorporate injury severity, procedures, transfer status, physiologic measures, discharge needs, and post-acute care pathways, helping distinguish whether residual geographic cost variation reflects clinical need, regional delivery-system organization, payment differences, or other factors.

A second extension is to move beyond 30-day costs. Firearm-injury survivors often require readmissions, rehabilitation, behavioral health care, durable medical equipment, prescription drugs, long-term services and supports, and caregiver time — and GAO has emphasized that information on long-term costs after firearm injury remains limited, especially beyond the first year after discharge. Future work should estimate longer-term costs and distinguish accounting costs from broader economic costs such as productivity losses, disability, and unmet care needs.

For Aim 2, future work should use finer temporal and geographic designs. Event-based or sub-annual analyses could test whether short-run supply disruptions produce different homicide responses than annual city-level averages. Larger panels and longer time horizons would improve precision, particularly for the opioid specifications. Additional mechanism tests could examine related outcomes — shootings, nonfatal assaults, overdose mortality, arrests, or emergency calls — to clarify whether market contraction, displacement, enforcement intensity, or organizational conflict is driving the observed association.

A cross-aim extension would test a question this dissertation does not answer: whether high-violence regions and high-cost treatment regions overlap more than expected by chance.

Such a study would require harmonized geography, clinical severity adjustment, and linked fatal and nonfatal injury data. It could examine whether the places with the highest violence burden are also the places where the health care system faces the highest per-patient treatment costs, or whether mortality selection, access barriers, referral patterns, and case mix separate those two geographies.

Methods-side extensions include nonstationary spatial fields that allow correlation length to vary by region, spatially varying coefficient models for the drug price–homicide relationship, and joint models that integrate firearm injury, overdose mortality, trauma-system access, and cost outcomes in a common spatial framework.

Conclusion

This dissertation yields three take-home messages.

First, firearm-injury treatment costs are locally uneven but regionally organized. Aim 1 estimated a county-level 30-day treatment-cost surface for treated firearm-injury patients and found that geographic inequality persisted after adjustment for local reimbursement geography, payer mix and insurance-market structure, demographic composition, injury burden, deprivation, local violence burden, health care capacity, and utilization norms. The residual variation should be interpreted cautiously. It may reflect regional delivery-system organization, unmeasured clinical need, injury severity, referral patterns, payer contracts, or some combination of these factors.

Second, higher instrumented drug prices were not associated with higher firearm homicide in the high-exposure cities studied. Aim 2 found negative point estimates across drug-price indices, with the clearest evidence in stimulant markets. These results are not a general endorsement of supply-side enforcement. They show that the violence effects of drug-price changes are empirical, setting-specific, and sensitive to model structure.

Third, spatial dependence is part of the substance of the problem. Both aims found geographic correlation at scales larger than the administrative units typically used for analysis. For costs, this points toward trauma systems, referral networks, and payment geography. For homicide, it points toward linked cities, trafficking corridors, and shared regional shocks. In both settings, methods that ignore spatial dependence risk missing the scale at which firearm-related harm is organized.

The dissertation's main contribution is not a final explanation of firearm violence or its costs, nor does it establish a unified causal pathway from illicit drug prices to firearm homicide to treatment spending. Its contribution is a framework for measuring two parts of the problem with greater geographic precision: the downstream treatment costs borne by patients, payers, hospitals, and public programs, and one upstream market condition that may shape lethal violence. The central lesson is that firearm-injury policy should be regional, financing-aware, and explicit about uncertainty. It should not rely only on national averages, isolated local estimates, or administrative boundaries that do not match the systems through which firearm-related harm occurs and is paid for.

References

1. United States Government Accountability Office. *Firearm Injuries: Health Care Service Needs and Costs*. GAO-21-515. Washington, DC: United States Government Accountability Office; 2021.